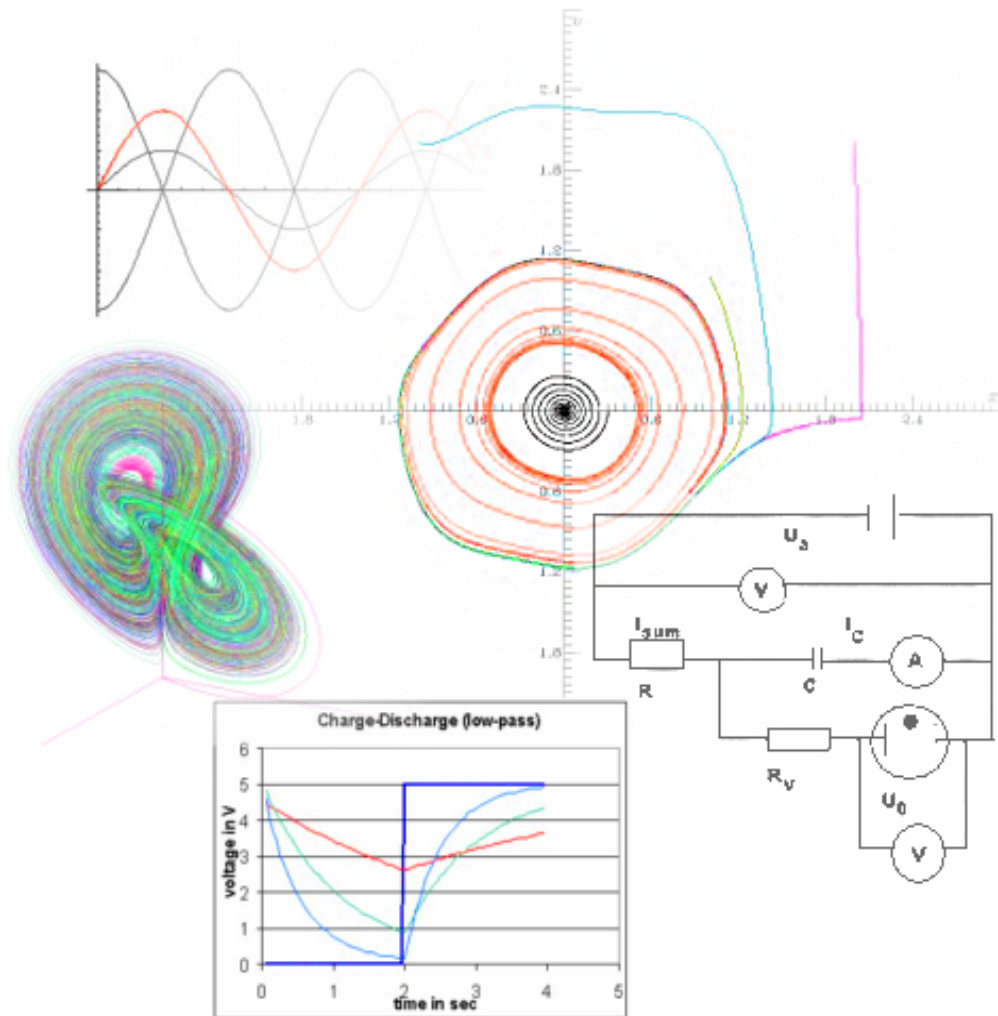Protocol on

Oscillations, Electricity,
and Chaos

by

Jens Ole Tietje, Thomas Unger,
Sebastian Schulz and Joachim Franck

Summer 2006

Contents

v3.1 (31st march, 2007)

I Introduction

Oscillating systems are defined as "systems with one or more physical parameters changing periodically in time". We divide between free oscillations, which work without interactions with their environment, and forced oscillations, which are influenced by an external force. Each real oscillation interacts with its environment by friction, which causes a damping of the oscillation's amplitude.

We can find oscillations almost everywhere in our environment: mechanical (pendulums, motors, clocks, bouncing balls, music instruments, rotation of planets around their stars), chemical (chemical reactions in "dynamic equilibrium", atoms in molecules), or biological ones (heartbeat, precision motion, prey-predator model). Oscillations can be described by their **amplitude** (maximum of the parameter's "deviation"), measured in relation to their **equilibrium point**, and **frequency** (or angular frequency, or period). If it is necessary to compare two oscillations with the same frequency, their **phase difference** is also important. Oscillation can only appear if there's an acceleration (force), pulling the system into the opposite direction of its deviation (for example a potential field). According to this, they can be described as a differential equation (DE) of 2nd order – acceleration depends on deviation and speed. Types of oscillations are:

In detail, the harmonic oscillator can be described by this differential equation

$$\ddot{x} + a \cdot x = 0 \qquad\qquad (I.1)$$

Its general solution is

$$x(t) = A cos(\omega t + \phi) \qquad\qquad (I.2)$$

where the constants A and Φ can be determined by the initial conditions x(0) and (dx/dt)(0).

In general you can say, the more complicated a DE of an oscillation is, the harder it can be algebraically solved. Those nonlinear equations have to be solved numerically and their corresponding systems are usually **sensitive to small perturbations of initial conditions** – chaotic. Examples are the double pendulum, the spring pendulum and the Lorenz system.

In this paper we will first analyze some electrical circuits and their elements in general to study the relationship between differential equations and their physical background. Then we will analyze two nonlinear (double pendulum and Lorenz system) systems numerically. At last we combine both by studying the Van der Pol oscillator – a nonlinear electrical circuit.

II Electronic circuits

II.1 Basic elements

In these series of measurement we analyse a resistor and different capacitors and coils.

II.1.1 Resistors

Electrical resistance is a measure of the degree to which an object opposes the passage of an electric current. The quantity of resistance in an electric circuit determines the amount of current flowing in the circuit for any given voltage applied to the circuit.

$$R = \frac{U}{I} \quad \text{and} \quad u_R = \left| \frac{1}{I} \cdot u_U \right| + \left| \frac{-U}{I^2} \cdot u_I \right| \quad \text{(measurement uncertainty)} \quad \text{(II.1.1)}$$

where
R is the resistance of the object, usually measured in ohms, equivalent to J·s/C^2
U is the potential difference across the object, usually measured in volts
I is the current passing through the object, usually measured in amperes
The u_i are the corresponding measuring-uncertainties.

For a wide variety of materials and conditions, the electrical resistance does not depend on the amount of current flowing or the amount of applied voltage. V can either be measured directly across the object or calculated from a subtraction of voltages relative to a reference point. The former method is simpler for a single object and is likely to be more accurate. There may also be problems with the latter method if the voltage supply is AC and the two measurements from the reference point are not in phase with each other.

We measured the voltage and the current for co-current flow in a current-right and a voltage-right measurement. Current-right measurements are used for high resistances, voltage-right measurements for low resistances. The measurement uncertainty is about 1% of the value.

Current-right: $U = (2{,}9 \pm 0{,}2)\,V$ $\qquad I = (34{,}1 \pm 0{,}7)\,\mu A$ $\qquad R_c = (85 \pm 8)\,k\Omega$

Voltage-right: $U = (2{,}9 \pm 0{,}2)\,V$ $\qquad I = (30{,}2 \pm 0{,}7)\,\mu A$ $\qquad R_v = (96 \pm 8)\,k\Omega$

II.1.2 Coils

In electrical engineering, an electromagnetic coil is formed when a metallic or conductive wire is looped around a core to create an electronic inductor or electromagnet. One loop of wire is usually referred to as one *turn*. A coil consists of one or more turns. For use in an electronic circuit, electrical connection terminals called taps are often connected to a coil. Coils have the property to have different resistances each for co-current flow – called active resistance – and alternative current – called impedance. The relationship between active resistance R and impedance Z is given by

$$Z = \sqrt{R^2 + X_L^2} \quad \text{or} \quad X_L = \sqrt{Z^2 - R^2} \quad \text{with} \quad u_{X_L} = \left| \frac{Z}{\sqrt{Z^2 - R^2}} \cdot u_Z \right| + \left| \frac{-R}{\sqrt{Z^2 - R^2}} \cdot u_R \right| \quad \text{(II.1.2)}$$

X_L is called the reactance of the inductor. The u_i are the corresponding measuring-uncertainties. We analysed coils with 750 and 500 turns.

co-current flow:
  500 *turns :* $U=(0{,}62\pm0{,}002)\,V$ $I=(0{,}11\pm0{,}03)\,A$ $R=(3{,}3\pm0{,}5)\,k\,\Omega$
  750 *turns :* $U=(0{,}99\pm0{,}002)\,V$ $I=(0{,}19\pm0{,}03)\,A$ $R=(8{,}8\pm0{,}9)\,k\,\Omega$

alternating current (with f = 50 Hz):
  500 *turns :* $U=(0{,}29\pm0{,}02)\,V$ $I=(0{,}0854\pm0{,}0005)\,mA$ $Z=(3{,}6\pm0{,}3)\,k\,\Omega$
  750 *turns :* $U=(0{,}74\pm0{,}02)\,V$ $I=(0{,}0818\pm0{,}0005)\,mA$ $Z=(9{,}0\pm0{,}3)\,k\,\Omega$

We then obtain   500 *turns :* $X_L=(1{,}4\pm1{,}0)\,k\,\Omega$
                      750 *turns :* $X_L=(1{,}9\pm1{,}1)\,k\,\Omega$

Now we can calculate the inductance L using the equation:

$$X_L \;=\; \omega L \;=\; 2\pi\cdot f\cdot L \quad\Leftrightarrow L \;=\; \frac{X_L}{2\pi\cdot f} \quad with \quad u_L \;=\; \left|\frac{1}{2\pi\cdot f}\cdot u_{X_L}\right| \tag{II.1.3}$$

and we obtain   500 *turns :* $L=(4{,}4\pm2{,}3)\,mH$
                     750 *turns :* $L=(6{,}0\pm2{,}5)\,mH$

The measurement uncertainty is quite big, but you can see, that inductors with more turns have a higher inductance than those with less turns.

II.1.3 Capacitors

A capacitor is an electrical device that can store energy in the electric field between a pair of closely spaced conductors (called plates). When voltage is applied to the capacitor, electric charges of equal magnitude, but opposite polarity, build up on each plate.

Capacitors are used in electrical circuits as energy-storage devices. They can also be used to differentiate between high-frequency and low-frequency signals and this makes them useful in electronic filters.

Capacitors also have a reactance at an alternative current. This reactance allows us to calculate the capacity by the equation:

$$Z \;=\; X_C \;=\; \frac{1}{\omega C} \;=\; \frac{1}{2\pi\cdot f\cdot C} \quad\Leftrightarrow\quad C \;=\; \frac{1}{2\pi\cdot f\cdot X_C} \quad and \quad u_C \;=\; \left|\frac{-1}{2\pi\cdot f\cdot X_C^2}\cdot u_{X_C}\right| \tag{II.1.4}$$

alternative current (with f = 2000 Hz):

  $C_1:$ $U=(2{,}496\pm0{,}005)\,V$ $I=(0{,}29\pm0{,}03)\,mA$ $Z=X_C=(8{,}6\pm0{,}9)\,k\,\Omega$
  $C_2:$ $U=(2{,}573\pm0{,}005)\,V$ $I=(0{,}66\pm0{,}03)\,mA$ $Z=X_C=(3{,}9\pm0{,}2)\,k\,\Omega$
  $C_3:$ $U=(2{,}695\pm0{,}005)\,V$ $I=(3{,}5\pm0{,}03)\,mA$ $Z=X_C=(0{,}8\pm0{,}1)\,k\,\Omega$

and so we obtain:

$$C_1 = (9,3 \pm 0,9)\,nF$$
$$C_2 = (20,4 \pm 1,1)\,nF$$
$$C_3 = (99,5 \pm 12,5)\,nF$$

Finally we can conclude that we can calculate the capacity by measuring the current and the voltage at an alternative current, the uncertainty is about 10%.

II.1.4 RCL Measuring bridge

All values calculated above, can also be measured directly by a RCL-measuring-bridge, which is used to measure an unknown electrical resistance by balancing two legs of a bridge circuit, one leg of which includes the unknown component. Its operation is similar to the original potentiometer except that in potentiometer circuits the meter used is a sensitive galvanometer. The measurement of the phase-difference allows the RCL-measuring-bridge, to calculate inductances and capacities directly. The measuring uncertainty is 1% + the last point of the value. The results are presented in the following table.

	calculated	*RCL-measuring-bridge*
Resistor	$R_c = (85 \pm 8)\,k\Omega$ $R_v = (96 \pm 8)\,k\Omega$	$R_c = (97 \pm 1)\,k\Omega$
Inductor with 500 turns	$L = (4,4 \pm 2,3)\,mH$	$L = (3,0 \pm 0,03)\,mH$
Inductor with 750 turns	$L = (6,0 \pm 2,5)\,mH$	$L = (6,0 \pm 0,06)\,mH$
Capacitor 1	$C_1 = (9,3 \pm 0,9)\,nF$	$C_1 = (9,1 \pm 0,1)\,nF$
Capacitor 2	$C_2 = (20,4 \pm 1,1)\,nF$	$C_2 = (20,9 \pm 0,3)\,nF$
Capacitor 3	$C_3 = (99,5 \pm 12,5)\,nF$	$C_3 = (99,5 \pm 1,5)\,nF$

All results are inside the measuring-uncertainty-interval, some values are even nearly exact. In the case of the resistor we can see, that the measured value with the voltage-right-switch is better than the other. This is due to the high resistance.

II.2 Capacitors in detail

II.2.1 Charge and discharge of a capacitor (manually)

Firstly we had to take a series of measurements for the voltage and the current on the charge and the discharge of a capacitor C = 100μF over a resistance R= 100 kΩ by measuring the values from an ammeter and a voltmeter.

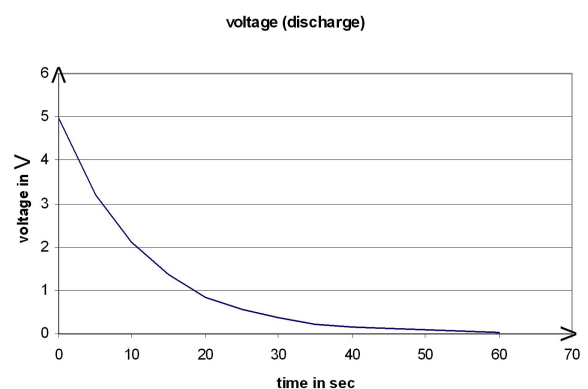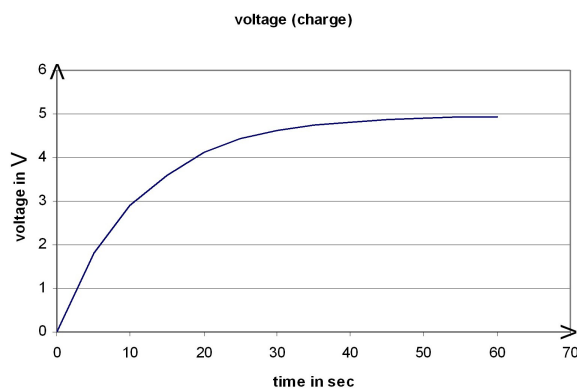| t in seconds (s)	charge		discharge		discharge over voltmeter
	U in Volt (V)	I in μA	U in V	I in μA	U in V
0	0,0063	44	4,97	-40	4,97
5	1,8	30	3,2	-32	4,92
10	2,9	21	2,1	-21,5	4,88
15	3,6	14,1	1,37	-13,4	4,84
20	4,14	9,5	0,84	-9,1	4,8
25	4,44	6,6	0,56	-6	4,76
30	4,63	4,76	0,36	-4,1	4,72
35	4,74	3,3	0,221	-2,4	4,68
40	4,81	2,5	0,162	-1,8	4,64
45	4,87	2,1	0,118	-1,3	4,6
50	4,9	1,7	0,081	-1	4,56
55	4,93	1,5	0,057	-0,6	4,52
60	4,94	1,3	0,042	-0,6	4,48
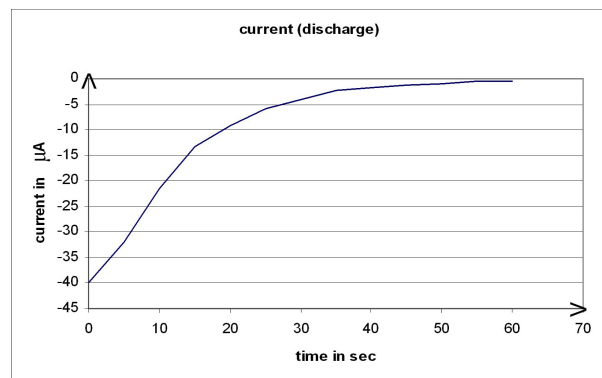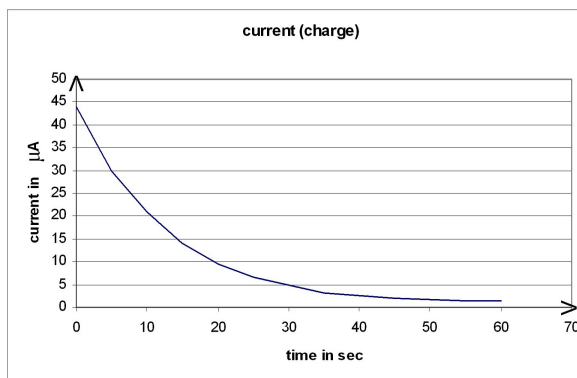
Fig. II.2.1: various charge and discharge curves of a capacitor

In Fig II.2.1 one see that the time of charge shows an exponential increase until the input-voltage of 5V nearly is achieved while the current-values are falling exponentially. When the capacitor is charged, it has the negative voltage as the input, but we define $U_o < 0$.

The equations for the charge-graphics for U and I are given by:

$$U(t) = -U_0 \cdot (1 - e^{\frac{-t}{RC}}) \quad \text{and} \quad I(t) = -\frac{U_0}{R} \cdot e^{\frac{-t}{RC}} \quad\quad\quad (\text{II.2.1})$$

The equation for the discharge is given by the exponential fall of U:

$$U(t) = -U_0 \cdot e^{\frac{-t}{RC}} \quad\quad\quad (\text{II.2.2})$$

The current flows during the discharge in the other direction, so it's negative. In this case the capacitor is the power supply of the electrical circuit, which the capacitor forms with the resistance. Because of the Kirchoff-law ($\Sigma U = 0$) and the relation $I = U_R/R$ we get the equation:

$$I(t) = \frac{U_o}{R} \cdot e^{\frac{-t}{RC}} \quad\quad\quad (\text{II.2.3})$$

Even in the switch position 0 there's a discharge, because the voltmeter in parallel is also a resistance (big but not endless). Fig II.2.2 shows that a discharge over a very big resistance nearly proceeds linear.
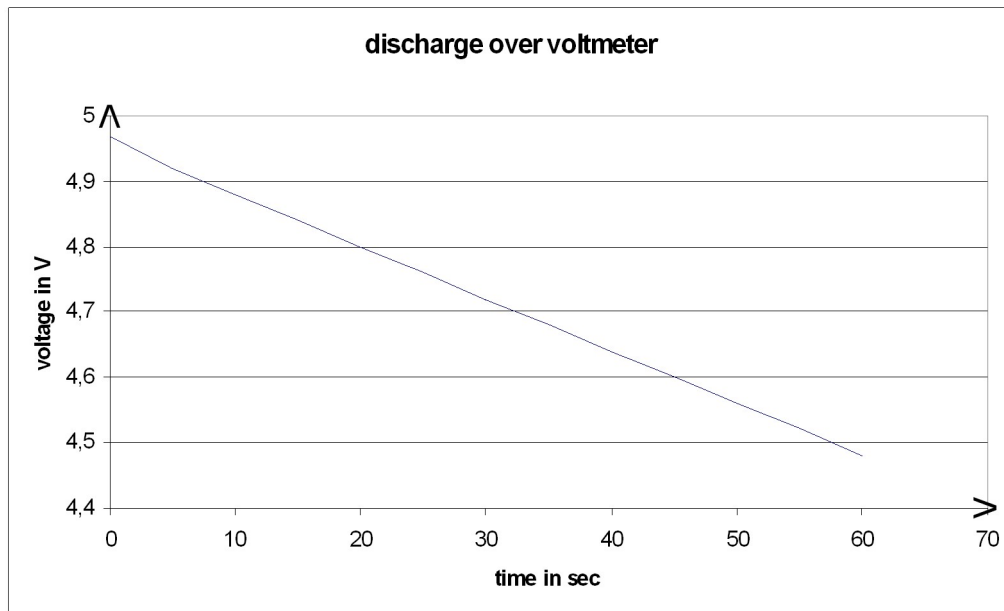

*Fig. II.2.2: Discharging a capacitor over a voltmeter*

We can say that the higher the resistance is, the slower the charge (or discharge) proceeds. (see also: different RC-elements)

II.2.2 Charge and discharge of a capacitor (by computer)

The next step is to measure the charge (discharge) of the same capacitor by a computer to get a graphic with very few mistakes, so we can measure the half-life of the discharging capacitor. By the half-life we can calculate the constant time $\tau = RC$:

For the half-life T_H we know that $U(T_H) = 0.5\ U_0$, so we obtain

$$\tau \;=\; \frac{T_H}{\ln 2}$$

Charge-Discharge-Diagram of a capacity
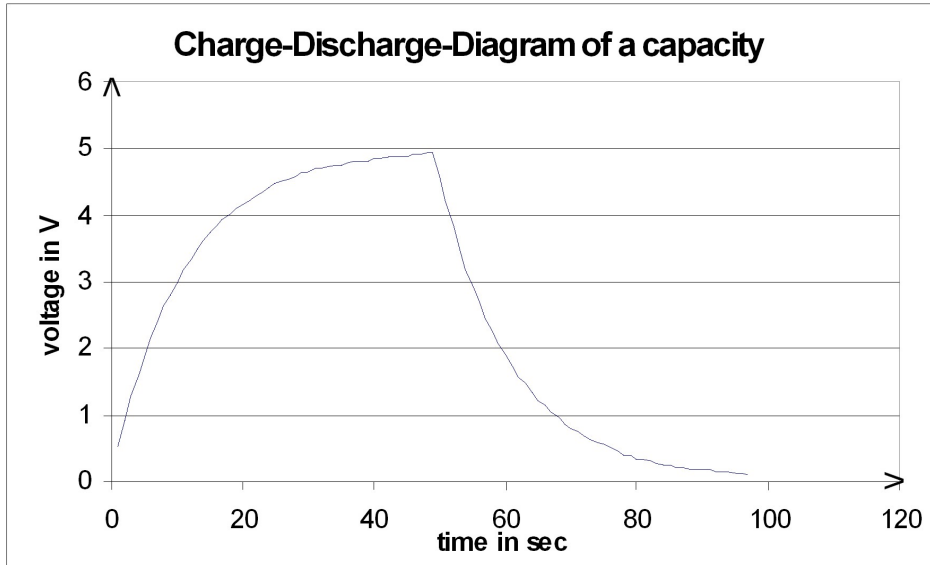
Fig. II.2.3: Charging and discharging a capacitor leads to logarithmic curves

(see appendix)

We get T_H by looking at the plot, so the risk of making measuring mistakes is big.
We get $T_H = 7.5$ sec. This means that we obtain $\tau = 10.8$ sec
Control: $\tau = RC = 100\ k\Omega \bullet 100\ \mu F \;= 10$ sec

Although our measuring process was slightly rough the result is quite good.

II.2.3 Output-voltage and displacement of phase for a low-pass filter

The characteristic of a low-pass filter is that sinusoidal voltages only pass for small frequencies of the input voltage. The smaller the frequency is the higher is the output voltage.

The capacitor has for sinusoidal voltages a reactance $X_C = 1/\omega C$ in such a way that

$$U_{output} \;=\; U_{input} \frac{X_C}{R + X_C} \tag{II.2.4}$$

The dimension-less transfer-function is: $|g(\omega)| \;=\; \dfrac{1}{\sqrt{1 + \omega^2 R^2 C^2}}$ (II.2.5)

8

We test this character of a low-pass filter with two input-frequencies (given is the period-time with T = 1/f): *with   T = 5 sec   and   T = 2.5 sec (R = 100 kΩ , C = 100 μF)*
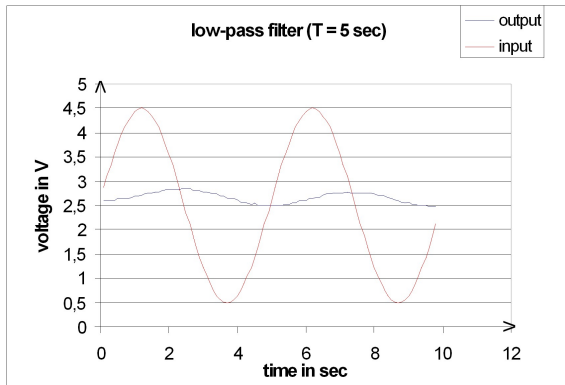

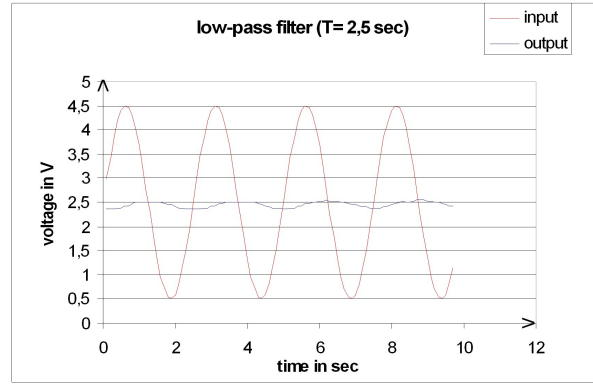Fig. II.2.4a: $\hat{U}_{out} = 0.15\ V$, $\Delta\Phi \sim \pi/2$ Fig II.2.4b: $\hat{U}_{out} = 0.1\ V$, $\Delta\Phi \sim \pi/2$

The resulting graphics (Fig. II.2.4a and b) show, that the output crest value for the higher frequency is smaller than the other. But at all, both are very small, so we guess, that the frequencies of both are not low enough. Also the displacement of phase is for both frequencies nearly exact $\pi/2$. The displacement of phase is positive because the output signal follows the input signal.

The displacement should become smaller for lower frequencies, but both are too high to see this relation exactly.

II.2.4 Output-voltage and displacement of phase for a high-pass filter

The characteristic of a high-pass filter is that sinusoidal voltages only pass for high frequencies of the input voltage. The higher the frequency is the higher is the output voltage.

The capacitor has for sinusoidal voltages a reactance $X_C = 1/\omega C$. We get

$$U_{output} \;=\; U_{input}\,\frac{R}{R + X_C} \tag{II.2.6}$$

The dimension-less transfer-function is: $|g(\omega)| \;=\; \dfrac{\omega RC}{\sqrt{1+\omega^2 R^2 C^2}}$ $\tag{II.2.7}$

We also test this property of a high-pass filter with two input-frequencies (given is the period-time with T = 1/f) (FigII.2.5 a and b).

We can see that the output crest value of the higher input-frequency is bigger than the other, and both are clearly bigger than the outputs of the low-pass filter. The displacements of phase are approximately $-\pi/3$ for T = 5 sec and $-\pi/4$ for T = 2.5 sec. The displacement of phase is negative because the input signal follows the output signal. We also see, that the displacement becomes smaller for higher frequencies.
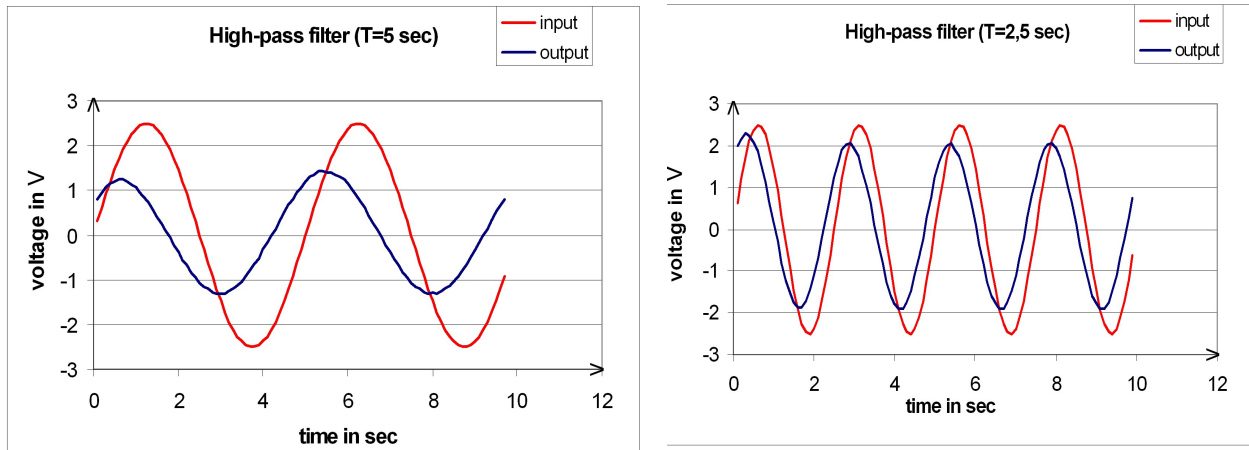
Fig II.2.5a & b: a high-pass filter (R = 100 kΩ, C= 100µF) with two different input-frequencies / period-times T = 1/f
(a) T = 5 sec
(b) T = 2,5 sec

II.2.5 Charge and discharge with different RC-Elements

We analyse the dependence of different RC-combinations for the charge and the discharge procedure by impressing a square wave voltage at a high-pass and a low-pass filter. This means a changing time-constant and a consequential different charge-discharge-behaviour.
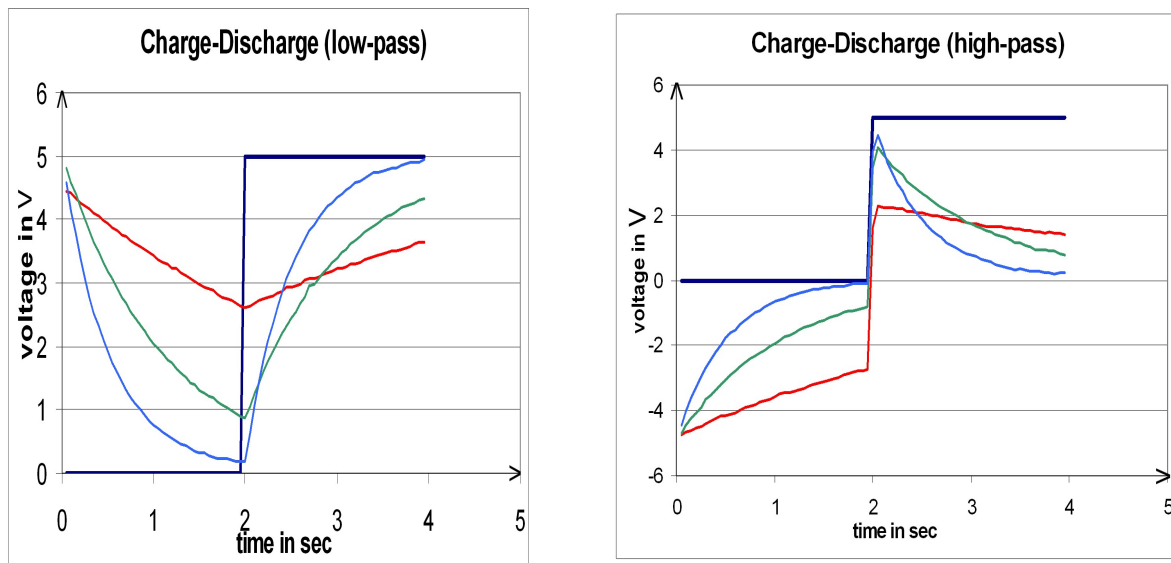

Fig. II.2.6: Charging and discharging a capacitor (C = 100µF) using different Resistors. Black: square wave voltage.   Blue: R = 4,7 kΩ. Green: R = 10 kΩ. Red: R = 33 kΩ.

The difference between high-pass and low-pass is, that at the low-pass we measure the voltage over the capacitor and at the high-pass over the resistance. So at the low-pass we see the normal plot of a capacitor-voltage for the charge-discharge procedure. The measurement of the high-pass results from the behaviour of the current, which is proportional to the voltage (U = R I) and which flows in different directions for the charge and the discharge, in both cases (charge-discharge) the current is high at the beginning and then decreases.

We also see the differences between the different RC-combinations. The capacitor charges (discharges) faster for smaller resistances, that's a behaviour we have already seen at the discharge over the voltmeter (Fig II.2.6), which has a very big resistance, similar to the red path (33 kΩ), which is nearly linear.

II.3 RCL serial circuit

In the first part of this experiment we investigate a serial circle by using of a two-channel-oscilloscope. Especially we have to show how the phase shift and the resistance depend on the supplied voltage frequency.

We realize this electrical circle with these special elements coil L, capacitor C, resistor R:
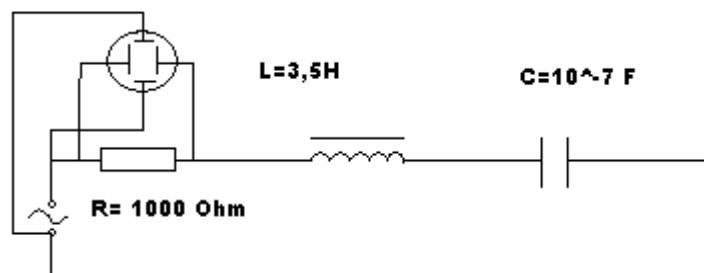

Fig. II.3.1: acceptor circuit diagram

We should also consider that the coil also has a resistance R_L which we measure with a normal multimeter to R_L=1500Ω so that we get a resulting resistance R_{sum}=R+R_L=2500Ω.

By changing the frequency within the range 200Hz ≤ f ≤ 500Hz the phase between the current, which is the same everywhere in the circle and the supplied voltage also changes. That is why the capacitor's voltage has a phase shift of -π/2 relatively to the current and the coil's voltage has a shift of π/2.

Using the oscilloscope we are able to measure the phase shift by counting the squares between two nearby peaks (one of the voltage over R (U_R) and one of the applied voltage U_0).

$$|\phi|=\frac{\Delta t}{T} \cdot 360\,°$$
(II.3.1)
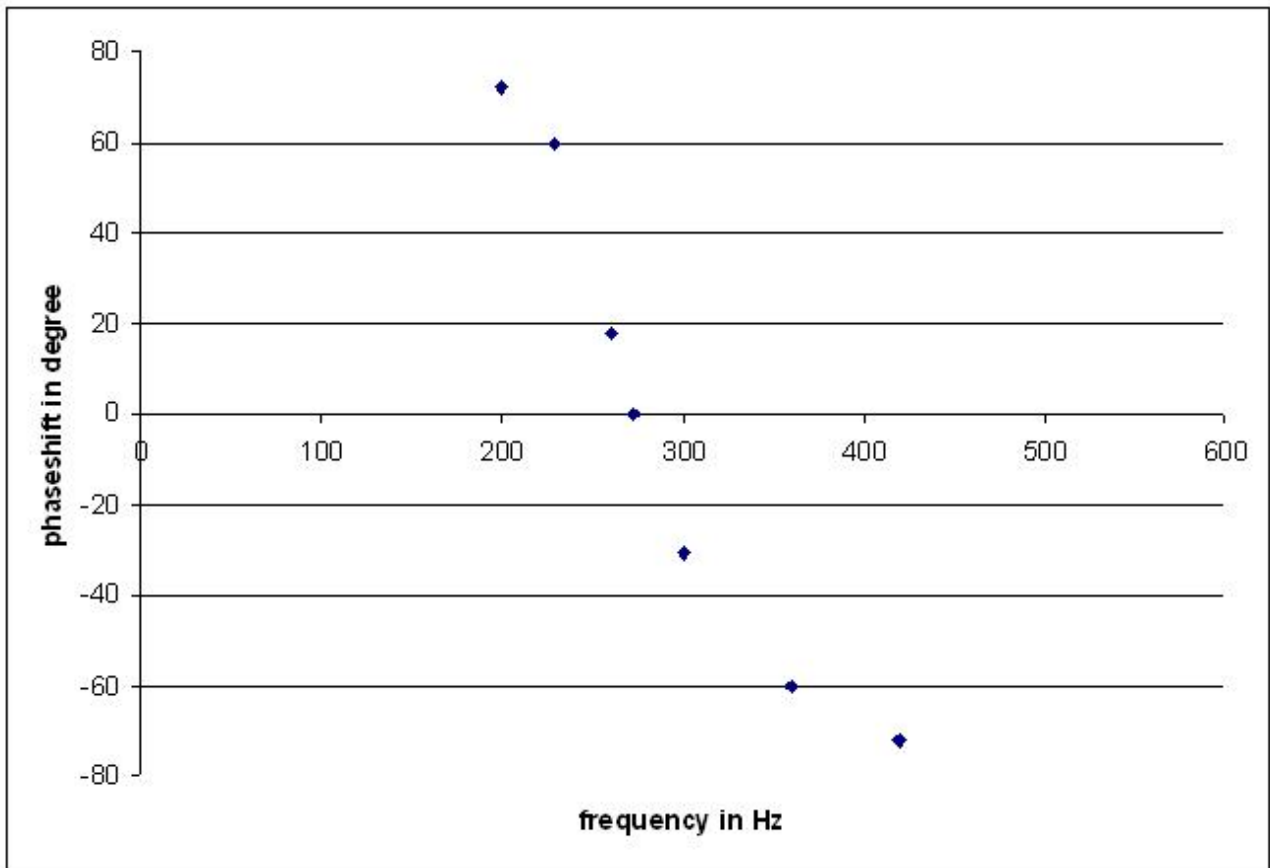
We can then plot the diagram:

Fig. II.3.2: phase shift diagram

As we can see the phase shift changes its signum because the capacitive resistance gets bigger than the inductive one. Hence the capacitive phase gets more important. Furthermore you can easily see that the zero point is at our measured resonant frequency at 273Hz.

The resistance of the whole circuit is called impedance Z. It consists of two parts: the reactive resistance X and the active resistance R. The reactive resistance consists of two parts itself: the capacitive X_C and the inductive resistance X_L.

$$Z=\sqrt{(X_L-X_C)^2+(R+R_L)^2}$$ (II.3.2)

Where $X_L=\omega\cdot L$ and $X_C=\dfrac{1}{\omega\cdot C}$.

To get the impedance experimentally we must divide the measured U_R by R. Since $i=i_R=i_l=i_C=\dfrac{U_R}{R}$, it follows that $Z=\dfrac{U_0\cdot R}{U_R}$ and we can plot the (Z,I)-diagram (fig. II.3.3).
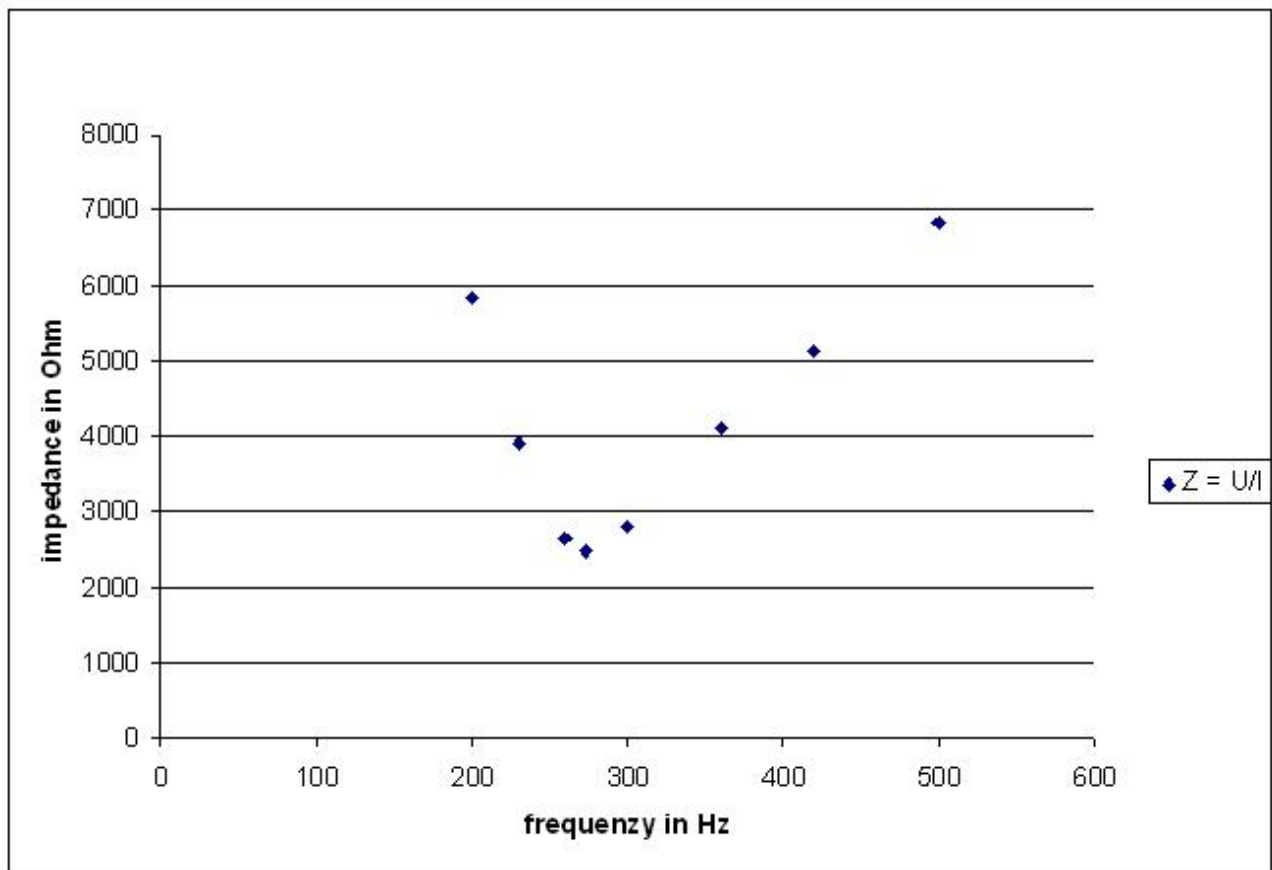
12

Fig.II.3.3: frequency dependence

We notice that there is a minimum of Z for our resonance frequency f_0 at about 270Hz. The graph should show a parabola, which we can approximately guess, but the right parabola branch doesn't rise as fast as the left one. The calculation of f_0 gives another value:

$$f_0 = \frac{1}{2\pi\sqrt{L \cdot C}}$$ (II.3.3)

With L=2.4H and C=10^{-7}F we obtain then f_0=324,9Hz. The reason of this difference is due to the fact that we have neglected the active resistance of the coil in the experimental process because we only measure the voltage dissipation U_R over the active resistance. The value obtained using the given equation doesn't need the active resistance of the coil.

Equally we obtain another value for our measured impedance in resonance case: $Z = 2484,8\,\Omega$ which is higher than the calculated resistance

$$Z = \sqrt{R^2 + \left(2\pi f_0 \cdot L - \frac{1}{2\pi f_0 C}\right)^2} = 1983,62\,\Omega$$ (II.3.4)

But if we replace R by R_{sum}=R+R_L the calculated impedance has the same value as the measured $Z \approx 2500\,\Omega$.

Even the voltage superelevation ϱ_U (the ratio of the voltages U_L and U picked off the input) reflects our previous results.

$$\varrho_U = \frac{U_{L,ss}}{U_{ss}} = \frac{I_{ss} X_L}{I_{ss} Z} = \frac{X_L}{Z} = \frac{\omega_0 L}{Z_{res}} = \frac{273\text{Hz} \cdot 134\text{H}}{11303\,\Omega} \approx 3,2$$ (II.3.5)

II.4 Anharmonic oscillations

We investigate here experimentally the relaxation oscillation, which is a kind of self-sustained oscillation. We use the following circle to investigate U(I):
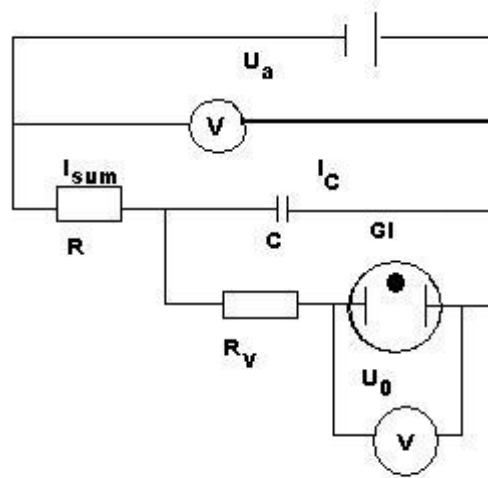

Fig. II.4.1: circuit diagram

Whereas U_a is a DC-power supply, C a capacitor, Gl is a glow lamp and Rv an integrated resistance of the glow lamp to reduce the current. The glow lamp starts to glow without a former current flow only at the ignition voltage U_i and the current immediately raises to the value I_i and gets more with the voltage. But if you lower the voltage the lamp goes out. The reason for this is found in the lamp's way of function.

If the voltage between them raises more electrons are emitted from the surface of the cathode and get a higher kinetic energy by the voltage: $eU = 1/2mv^2$. At a special voltage U_i the kinetic energy of the emitted electrons is high enough to ionise gas atoms and free more. So if they are available, the current flow also increases because of the ionisation of electrons and ions recombine under emission of photons. But there are also ionisation caused by impacts, which also heat the gas. That is why the lamp is still glowing at a voltage lower than the starting value.

We can create electrical oscillations because of the difference between the starting and expiration voltage: If we put a voltage on the circle the capacitor begins to charge with:

$$U_c = U\left(1 - e^{-tRC}\right)$$ (II.4.1)

As soon as the voltage at the capacitor reaches the starting value U_i, it begins to discharge over R_v nearly instantaneous as long as U_c descreases to the value of expiration. Then the capacitor starts to recharge until the voltage reaches ignition value again.

The mesh law tells us that:

$$I_c + I = 0$$ (II.4.2)

$$I_c = C\dot{U}$$ (II.4.3)

$$R_v I + U_0 = 0$$ (II.4.4)

We get the differential equation by putting eq. (II.4.2) in (II.4.3) and dividing it by C:

$$\dot{U} + \frac{1}{R_v C}(U - U_0) = 0 \tag{II.4.5}$$

Separating the differentials of dU/dt so that we can integrate the whole equation:

$$\int_{t_0}^{t_e} \frac{-dt}{R_v C} = \int_{U_{(0)}}^{U_e} \frac{dU}{U - U_0} \tag{II.4.6}$$

integration delivers:

$$\frac{-t_e}{CR_v} + \frac{t_0}{CR_v} = \ln(U_e - U_0) - \ln(U(0) - U_0) \tag{II.4.7}$$

Now we set $U(0) = U_Z$ and $U_e = U_L$ putting each side in the exponential function and solve for U_L.

$$U_L = U_0 + (U_Z - U_0)e^{\frac{-t_e}{CR_v}} \tag{II.4.8}$$

$$t_e = C \cdot R_v \ln\left(\frac{U_Z - U_0}{U_L - U_0}\right) \tag{II.4.9}$$

For the charging process we have the conditions: $U(t_e) = U_L$ is the initial condition, $I_{sum} = I_C = C\dot{U}$ and Ua = R I_{sum} + U_C. We get the differential equation:

$$\dot{U} + \frac{1}{RC}(U - U_a) = 0 \tag{II.4.10}$$

By separation of the variables and following integration between the values of time (t_a and 0) and corresponding values: U_z and U_l. So we are able to calculate the charging time t_a in the same way in (II.4.9).

$$t_a = RC \ln\left(\frac{U_a - U_Z}{U_a - U_l}\right) \tag{II.4.11}$$

$$T = t_e + t_a \tag{II.4.12}$$

Firstly we measure in our experiment the starting voltage and expiration voltage to U_i = 142V and U_e = 130V . After that we put an amperemeter in the circle to obtain the characteristic (I, U). The regression equation is: U=0,019*I+126,85. It tells us that U_0 = 126.85V and R_v = 19kΩ. Then we have examined the period time in dependence of several RC combinations.

What we expect is that for a constant capacitor and a small resistance the charge current is high and consequently there is only a short time for charging. Whereas a bigger resistance or a larger capacity causes a larger time because of a lower current.

In order to receive reliable measured values for the period time we measure the time necessary for 10 periods for each RC-combination and take the average value and compare it with the value we get using equation (II.4.12).

If we take into account that there are many different measured voltages playing a role, all connected with their own failures gaining importance, our calculated and measured values must be near by the real ones.
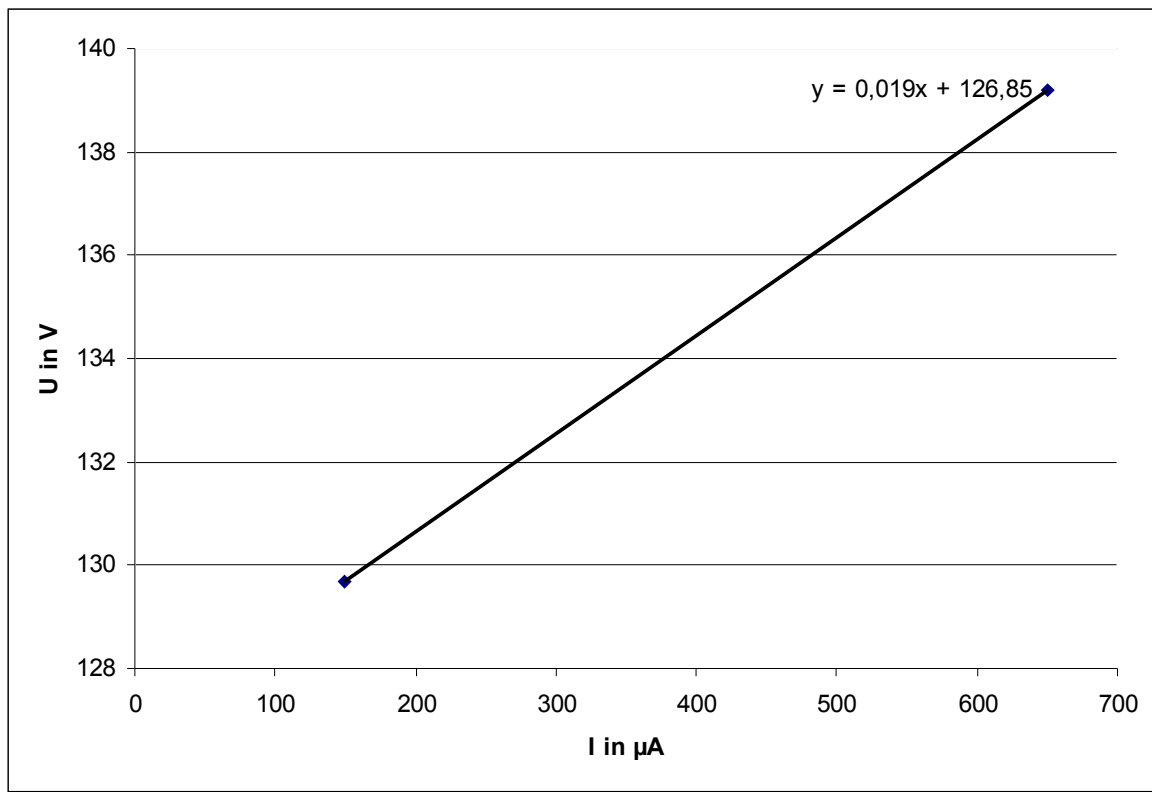

Fig. II.4.2: (I, U) characteristic

III Dynamic systems

III.I Introduction to chaos

Chaotic systems have one main property: For initial values lying very close together, the trajectories originating from these values diverge exponentially in time. That means these systems are sensible to small perturbations of initial conditions.

This fact was famously published by Lorenz. He said: "As small a perturbation as a butterfly fluttering its wings somewhere in the Amazons can in a few days time grow into a tornado in Texas" (Nonlinear Dynamics, M. Lakshmanan, S. Rajasekar, Springer 2003, p.101).

Some systems with a chaotic behaviour was already known in the 17th century like turbulences occurring when water circumflues for example stones in little rivers. But calculus to describe those systems was still in development in those days.

In the early 20th century, mathematical questions of stability (and first solutions), for example of our solar system were focused by famous mathematicians and physicians. Henri Poincaré said that "there are high complex motions nearby unstable fix points and that's why two curves in phase space have to cross arbitrarily often."
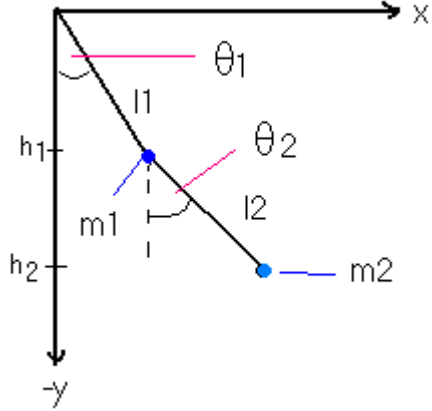
Other famous people who worked on chaotic systems were George Birkhoff, who solved dynamical problems with help of coordinate transformations and who introduced the so called Birkhoff coordinates, Lyapunow (Lyapunow exponent) and in astrophysics Kolmogorov, Arnold and Moser (KAM theorem that uses methods of topology). The KAM theorem, especially, divides systems into chaos and stability. Moser's proof of this theorem already includes an important geometric object for analysing chaos: the torus. He looked for invariant curves of area preserving mappings of an Annulus.

Today one tries to simulate chaos with the help of computer simulations. Not only faster computers but also especially better numerical methods can show how chaos and order coexist. Comparing the Newton approximation procedure with nowadays ones, one can show, that they can solve problems in 1 second for which Newton needs 21000 years. In our numerical calculations with the dynamical solver we used the Runge Kutta 8 procedure.

With help of these new methods, it has been found numerically, as predicted by KAM, that our solar system will be stable for the next 5 billion years. Before these new methods of computation one could make predictions for only a few million years. But nevertheless it is still difficult to decide whether the chaos one simulates is caused by the rounding errors in the simulations itself or is a physical reality.

III.2 Double pendulum

We observe a double pendulum where the rods are mass less. Thus only the two masses at the end of the rods with the coordinates (x_1,y_1) and (x_2,y_2) have masses m_1 and m_2. The rods have the lengths l_1 and l_2. Analogue to Fig. III.2.1 we can set the equations:

$$
\begin{aligned}
x_1 &= l_1 \cdot \sin(\theta_1) \\
y_1 &= -l_1 \cdot \cos(\theta_1) \\
x_2 &= l_1 \cdot \sin(\theta_1) + l_2 \cdot \sin(\theta_2) \\
y_2 &= -l_1 \cdot \cos(\theta_1) - l_2 \cdot \cos(\theta_2)
\end{aligned}
\qquad \text{(III.2.1)}
$$

Fig. III.2.1: Cartesian coordinate system with
the position of the two rods

With help of the generalised coordinates θ_1 and θ_2 we can plot the behaviour of our system by using the Lagrange equations:

$$
\frac{d}{dt}\frac{\partial L}{\partial \dot{\theta}_i} - \frac{\partial L}{\partial \theta_i} = 0
\qquad \text{(III.2.2)}
$$

Therefore we need the velocities, which we obtain by differentiating equations (III.2.1):

$$
\begin{aligned}
\dot{x}_1 &= l_1 \cdot \dot{\theta}_1 \cdot \cos(\theta_1) \\
\dot{y}_1 &= l_1 \cdot \dot{\theta}_1 \cdot \sin(\theta_1) \\
\dot{x}_2 &= l_1 \cdot \dot{\theta}_1 \cdot \cos(\theta_1) + l_2 \cdot \dot{\theta}_2 \cdot \sin(\theta_2) \\
\dot{y}_2 &= l_1 \cdot \dot{\theta}_1 \cdot \sin(\theta_1) + l_2 \cdot \dot{\theta}_2 \cdot \cos(\theta_2)
\end{aligned}
\qquad \text{(III.2.3)}
$$

The potential energy is given by:

$$
V = m_1 g h_1 + m_2 g h_2
\qquad \text{(III.2.4)}
$$

whereas h_1 and h_2 can be expressed analogue to fig. III.2.1 by generalised coordinates:

$$
\begin{aligned}
h_1 &= l_1 \cos\theta_1 \\
h_2 &= l_1 \cos\theta_1 + l_2 \cos\theta_2
\end{aligned}
\qquad (III.2.5)
$$

Thus we get as Langrangian:

$$L = T - V \tag{III.2.6}$$

$$L = \tfrac{1}{2}\, m_1 * (l_1 \dot\theta_1)^2 + \tfrac{1}{2}\, m_2 * ((l_1 \dot\theta_1)^2 + (l_2 \dot\theta_2)^2 + 2l_1 l_2 \dot\theta_1 \dot\theta_2 \cos\theta_1 \cos\theta_2$$
$$+ 2l_1 l_2 \dot\theta_1 \dot\theta_2 \sin\theta_1 \sin\theta_2) + (m_1 + m_2)gl_1 \cos\theta_1 + m_2 gl_2 \cos\theta_2 \tag{III.2.7}$$

Using Lagrange equations (III.2.2) and setting in (III.2.3) – (III.2.7) we get:

$$m_2 l_2(g\sin\theta_2 + l_2 \ddot\theta_2 + l_1 \ddot\theta_1 \cos(\theta_1-\theta_2) - l_1 \dot\theta^2_1 \sin(\theta_1-\theta_2)) = 0$$
$$l_1((m_1+m_2)(g\sin\theta_1 + l_1 \ddot\theta_1) + m_2(l_2 \ddot\theta_2 \cos(\theta_1-\theta_2) + l_2 \dot\theta^2_2 \sin(\theta_1-\theta_2))) = 0 \tag{III.2.8}$$

These two homogeneous differential non-linear equations describe the motion of the double pendulum.

III.2.1 Small angles

Small angles are valid for: $\sin\theta \approx 0$ and $\cos\theta \approx 1$. That's why for small elongations the equations can be dealt nearly linearly:

$$m_2 l_2(l_2 \ddot\theta_2 + l_1 \ddot\theta_1) = 0$$
$$l_1((m_1+m_2)l_1 \ddot\theta_1 + m_2 l_2 \ddot\theta_2) = 0 \tag{III.2.9}$$

We have checked these predictions with the program for small angles and for small differences concerning the angles. The behaviour of the system is not chaotic analogue to our results in equation III.2.9 and that's why small differences in initial values effects small differences in the course of time.

To illustrate this we have chosen $x_{11} = 0{,}3$ and $x_{12} = 0{,}31$ as initial values (with $x_{21} = x_{22} = 0{,}3$). The velocities are $v_1(t=0)=0$ and $v_2(t=0)=0$ (like in all calculations in paragraph II.2). As one can see the graphs in the (t,x)-diagrams are congruent. The red lines of 0,3 in the two diagrams are right above of these of 0,31. These plots of $x_1(t)$ and $x_2(t)$ look approximately like the sinus function (see Fig. III.2.2 and Fig. III.2.3). We have also plotted the phase space (Fig. III.2.4). One can see very well that the lines move on the surface of a torus.
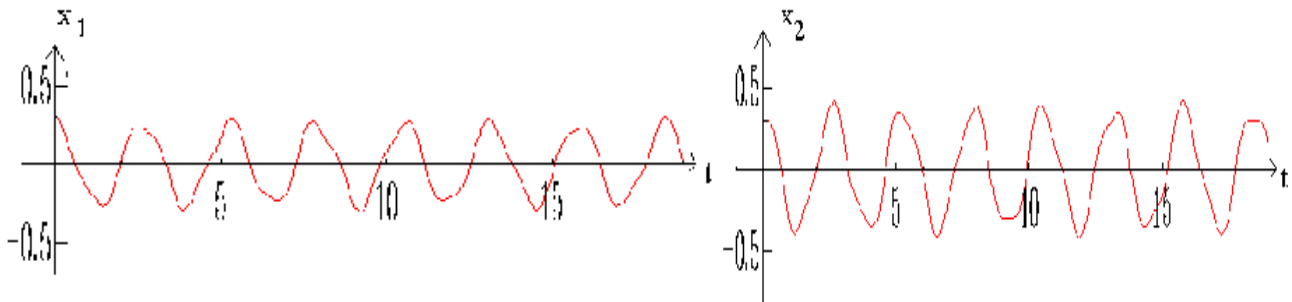

Fig. III.2.2 and III.2.3: (t,x_1)- and (t,x_2)-diagram for the initial values $x_{11} = 0{,}3$ and $x_{12} = 0{,}31$, $x_{21} = x_{22} = 0{,}3$
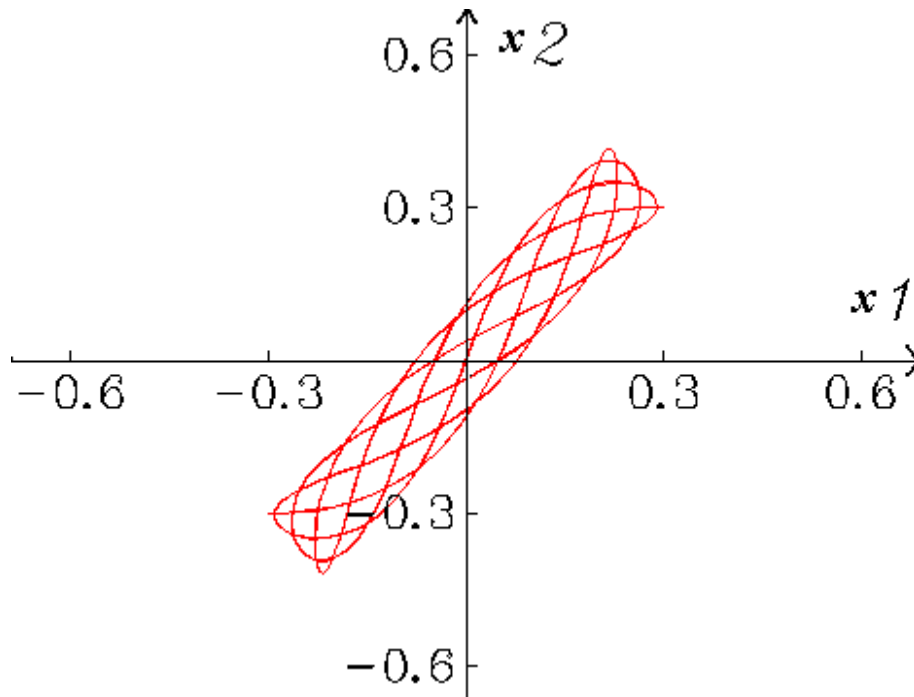
Fig. III.2.4: phase space for the initial values $x_{11} = 0,3$ and $x_{12} = 0,31$, $x_{21} = x_{22} = 0,3$

III.2.2 Large angles

For larger angles we have to plot the system for the non-linear differential equations without a linear approximation. Thus there is a distinct chaotic behaviour as one can also see in Fig. III.2.6 compared with the harmonic behaviour for small angles in Fig. III.2.5.
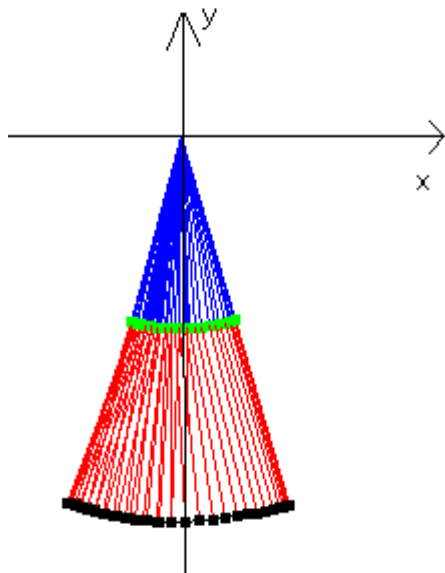

Fig. 3.5: Movement of the double pendulum inserted in an x – y coordinate system with initial conditions $x_1 = 0.3$ and $x_2 = 0.3$
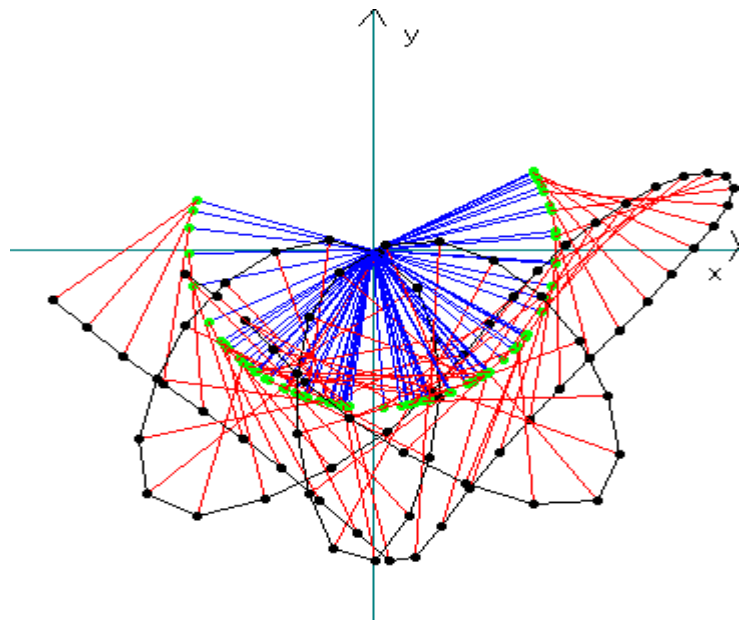
Fig. 3.6 : Movement of the double pendulum inserted in an x – y coordinate system with initial conditions $x_1 = 1.8$ and $x_2 = -0.4$

We have chosen $x_{11} = 1,8$ and $x_{12} = 1,8001$ as well as $x_2 = -0,4$ (for both cases) as initial conditions. The values are very close together and the system firstly moves nearly congruent as you can see in Fig. III.2.7 and in Fig. III.2.8 where the green line ($x_{12} = 1,8001$) covers completely the red line ($x_{11} = 1,8$) until t ≈ 20. Then a diverged motion starts. That's the mentioned main property of chaotic systems. You can also see in Fig. III.2.7 that the movement is complex: The two rods seem to "increase themselves" so that you can watch multiple flashovers of the second rod in both directions. But nevertheless one can notice a certain regularity within the chaos by looking figures III.2.7 and III.2.8: Watching the green lines in both diagrams you can observe repeating curve shapes.
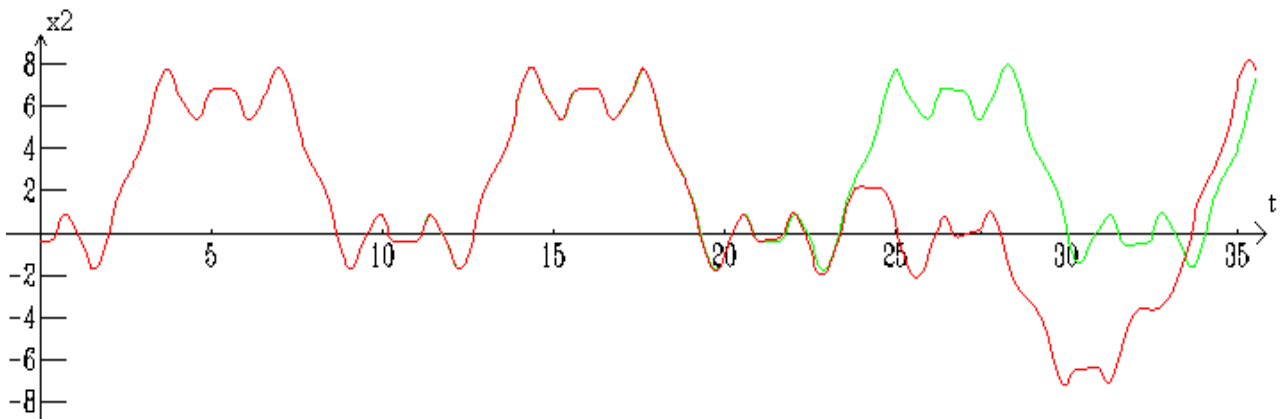

Fig. III.2.7: Variation of x_2 as function of time t for initial conditions $x_{11} = 1,8$ and $x_2 = -0,4$ (red line) and
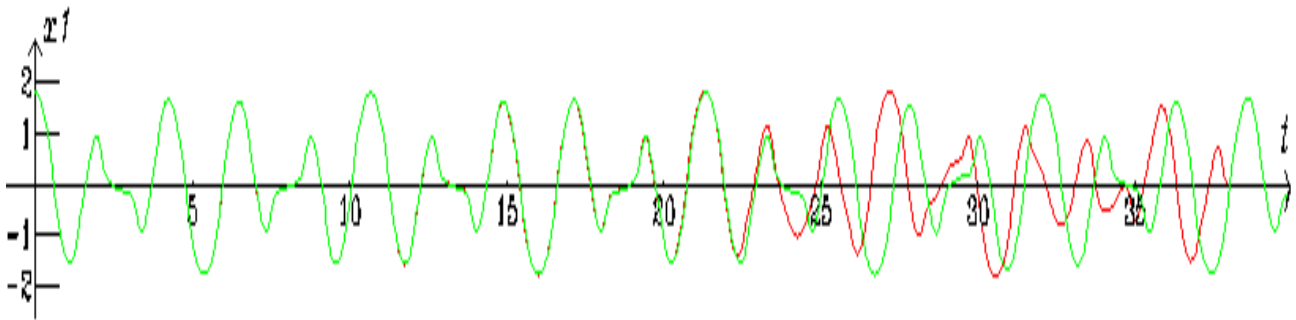$x_{12} = 1,8001$ (green line)

Fig. III.2.8: Variation of x_2 as function of time t for initial conditions $x_{11} = 1,8$ and $x_2 = -0,4$ (red line) and
$x_{12} = 1,8001$ (green line)

But one can also set $x_1 = 2$ and $x_2 = 2$ as initial conditions. In Fig. III.2.9 it is not possible to see the previously mentioned regularity. The motion seems to be completely uninfluenced by events happened earlier in its curve shape. And thus the graph in the phase space (Fig. III.2.10) can't be associated with a certain geometric object like a torus. It seems that the torus has bursted and now the graph is moving irregularly in the phase space. That means even conservative and easy systems like the double pendulum contains chaotic motion.
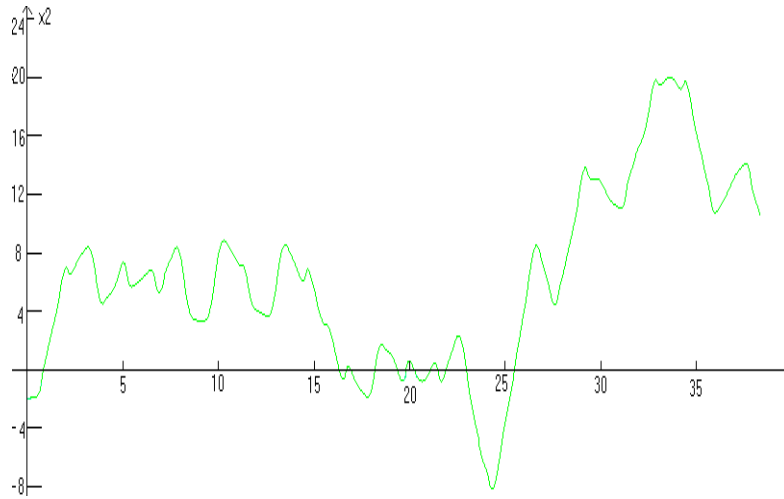
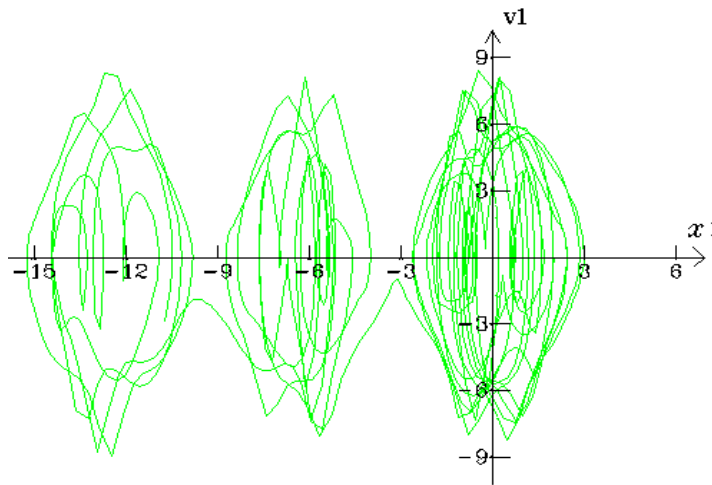Fig. III.2.9: Variation of x_2 as function of time t for initial values $x_1 = 2$ and $x_2 = 2$

Fig. III.2.10: Phase space for initial values $x_1 = 2$ and $x_2 = 2$

III.3 The Lorenz system

Another example of a system presenting chaotic behaviour is the Lorenz system. It was proposed in 1963 by Ed Lorenz to describe convection of air in a vertical loop and is given by the following set of 3 ordinary differential equations:

$$\dot{x} = s*(y\text{-}x)$$
$$\dot{y} = rx - y - xz \qquad\qquad (III.3.1)$$
$$\dot{z} = xy - bz$$

x, y, z are the variables and r, s and b are the parameters. The nonlinearities are in the second and third equation because of the terms xz and xy.

III.3.1 Physical Meaning

We can imagine a layer including a fluid dynamical system that is heated from the inferior surface. It results a temperature difference between the top and the bottom. Thus, corresponding to the Navier Stokes equations, we get a convectional motion in the layer. This motion (Fig. III.3.1) shall be described by our model.
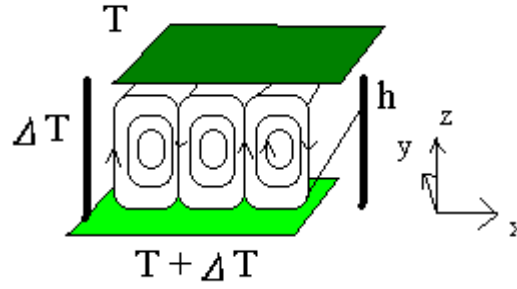
Fig. III.3.1: convection roles caused by a temperature difference

The mathematical basis is given by the following equations:

Continuity equation – conservation of mass:

$$\frac{\partial \rho}{\partial t} + div(\vec{\rho v}) = 0 \tag{III.3.2}$$

Navier Stokes equation – conservation of momentum:

$$\rho \frac{\partial v}{\partial t} = \rho \frac{dv}{dt} + \rho(\vec{v} \cdot \vec{\nabla})\vec{v} = \vec{\rho g} - \nabla p + \eta \nabla^2 \vec{v} \tag{III.3.3}$$

Heat transmission equation – conservation of energy:

$$\frac{\partial T}{\partial t} = \left(\frac{\partial T}{\partial t} + (\vec{v} \cdot \nabla)T \right) = \frac{\lambda}{\rho c_v} \nabla^2 T \tag{III.3.4}$$

One assumes: The density of the incompressible fluid is constant in whole the system and in time and is independent of pressure and linearly dependent of temperature. The convection roles have an endless extension in y direction.

With these assumptions and a long calculus one can reduce equations III.3.2-4 to the set of equations III.3.1, where:

$s = \dfrac{\eta \; c_v}{\lambda}$ is the Prandtl number. It specifies the inertia of the hydrodynamic system. For very large s-values the system has no inertia and thus the temperature changes instantaneously.

$b = \dfrac{4}{1 + a^2}$ with $a = \dfrac{height \; of \; one \; cell}{width \; of \; one \; cell}$ describes the cell shape.

$r = \dfrac{Ra_{crit}}{Ra}$ with $Ra = \dfrac{\rho g h^3 \Delta T c_V \alpha}{\lambda v}$ and $Ra_{crit} = \dfrac{\pi^4 (1 + a^2)^3}{a^2}$

is the relative Rayleigh number. This number refers to the heat transfer within the fluid. Below the critical Rayleigh number it's primary in the form of conduction, above in the form of convection. Furthermore x(t) is proportional to the intensity of convection current, y(t) represents the temperature difference and z(t) is proportional to the variation of the linear temperature profile.

III.3.2 General characteristics

To characterize what happens theoretically in this system we firstly look for equilibrium points. These points can be calculated by setting the first derivatives equal to zero. We get:

$$x = y = \pm\sqrt{b(r-1)} \qquad\qquad\qquad (III.3.5)$$
$$z = r - 1$$

Furthermore the sum of the first derivatives of the right sides says whether a system is conservative (total mechanical energy is conserved) or dissipative:

$$\nabla\cdot F \;=\; \frac{\partial}{\partial x}\;(s*(y\text{-}x)) + \frac{\partial}{\partial y}\;(rx - y - xz) + \frac{\partial}{\partial z}\;(xy - bz) \;=\; - (s + b + 1) \qquad (III.3.6)$$

In the following we set $b = 8/3$ and $s = 10$ (standard case of the Lorenz system; in general s and b are set bigger than 0) for all calculations with the dynamic solver. Thus the observed system is dissipative that means that the phase space volume isn't preserved in contrast to conservative systems that preserve the phase space volume according to Liouville's theorem.

Furthermore we fix the initial conditions:$x = y = z = 20$. These constraints are necessary because in this case we don't want to study effects occurring while changing initial values but the influence of a parameter r, on the system's behaviour.

III.3.3 r – variation

III.3.3.1 r = 0,5 < 1 and origin as equilibrium point

We can see that the oscillation of the system is damped strongly so that the graph points at the origin (see Fig. III.3.2), the first stable point, that can be concluded by symmetry reasons. One can also see that we have no other equilibrium points in the real space because *(r-1) < 0* and that's why the root is imaginary. These results can be seen in Fig. III.3.3. Referring to the physical meaning from section III.3.2 one can determine that convection doesn't take place in this case.
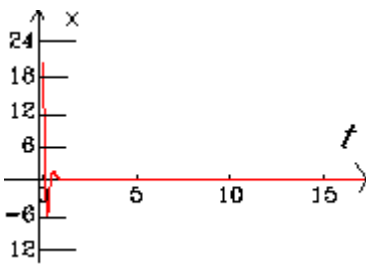

Fig. III.3.2 variation of x as function
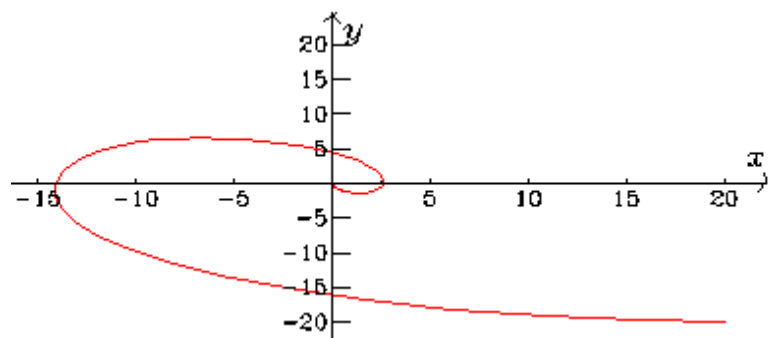of t for initial conditions
(x, y, z) = (20,20,20) ; r = 0,5

Fig. III.3.3 (x, y)-diagram for initial conditions
(x, y, z) = (20,20,20) ; r = 0,5

III.3.3.2 r = 5 > 1 and pitchfork bifurcation

For this case we observe that the oscillation is damped, too. But for r > 1 we have two new equilibrium points. With equation (III.3.5) we get:

$$x = y = \pm\sqrt{\frac{32}{3}} \quad \text{and } z = 4 \qquad\qquad \text{(III.3.7)}$$

This creation of two new stable points is called a pitchfork bifurcation. It appears in pairs in symmetric systems. It tends to appear in the Lorenz system because of the spatial symmetry between left and right side concerning the z-axis. At a threshold of r the axial position mentioned in III.3.3.1. becomes unstable and the two new stable points are born. Calculating it mathematically by the eigenvalue equation is presented in section III.3.3.5. when we also elaborate on other types of bifurcations occurring for different r-values.
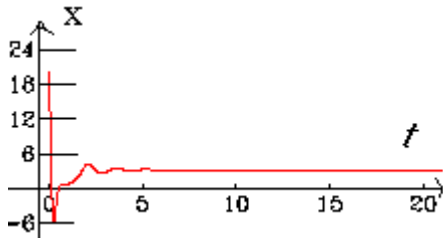

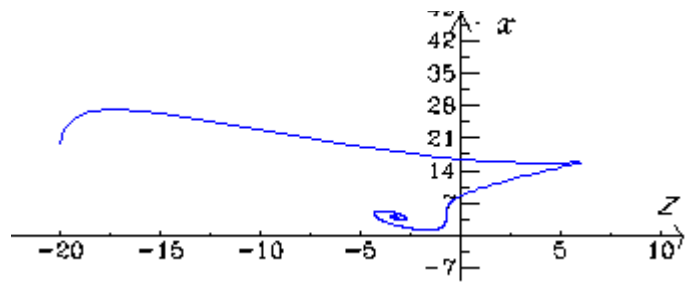Fig. III.3.4: One can read off the stable point coordinate x ≈3,3 in the (t, x)-diagram analogue to equation (III.3.4)

Fig. III.3.5: One can read off the stable point coordinates x ≈3,3 and z = 4 in the (z, x)-diagram analogue to equation (III.3.4)

III.3.3.3 r = 23.498 and instable spirals

For this value of r we can detect the system's transient between the two stable points. The chaotic behaviour can be seen in figure III.3.6: The systems oscillates with an incessantly changing number firstly around the first stable point than around the other one and again backwards. Finally at t ≈ 1000 the movement finishes at one stable point (straight line at the right hand side of the diagram). This seems to indicate at a special point in the chaotic system, another bifurcation, were its behaviour changes from stable points to stable spirals around these points.
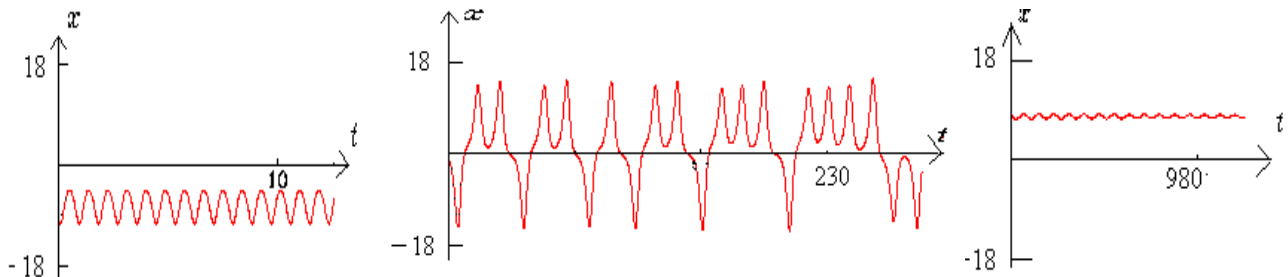

Fig III.3.6 a-c: These (t, x)-diagrams show that even after some hundred seconds oscillating around the stable points the system can seemingly abrupt stop oscillating and converge at one stable point.

III.3.3.4 r = 24.1 and influence of initial conditions

Because of the transitional stage of the system in this interval focus on initial values variation and let r = 24.1. The first set is (x, y, z) = (20, 20, 20) , the second one is (x, y, z) = (1, 5, 0).

As you can see in Fig. III.3.9 and Fig. III.3.10 we have two different behaviours: For our standard initial values we see two attractive points. But for the other set of initial values we still have 1 equilibrium points as we had for lower values of r. This situation can also be seen in figures III.3.7 and III.3.8. In figure III.3.8 the motion stops at t≈290.
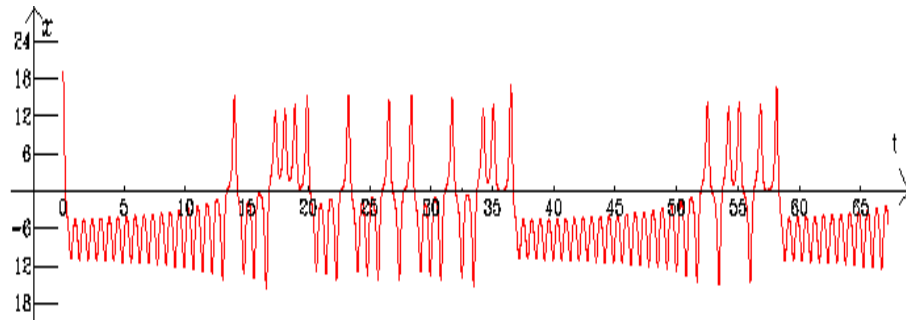

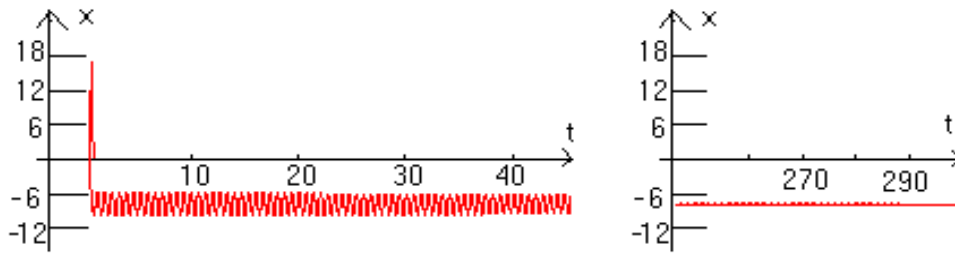Fig. III.3.7: variation of x as function of t for   initial values (x, y, z) = (20, 20, 20)

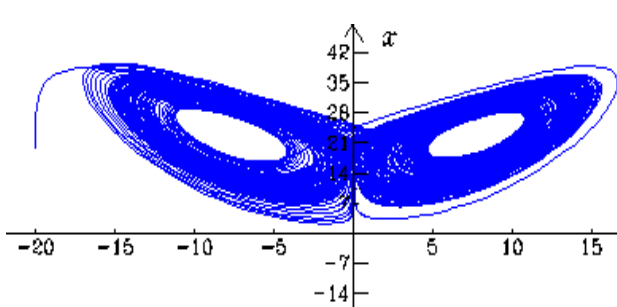Fig. III.3.8a and III.3.8b: x as function of t for initial values (x, y, z) = (1, 5, 0)

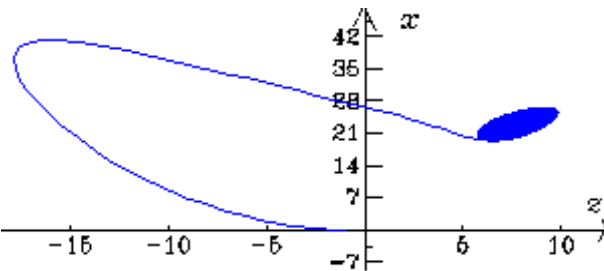Fig. III.3.9: (z,x) - diagram for initial values (x, y, z) = (20, 20, 20)

Fig. III.3.10: (z,x) - diagram for initial values (x, y, z) = (1, 5, 0)

III.3.3.5 r = 24.74, r = 24.74001 and Hopf bifurcation

Regarding these two values of r we want to show two aspects typically for chaos. The first one refers to our definition. We have mentioned that very small perturbations affect the system. One can agree that by changing the values of parameters the trajectories can also diverge. We can't observe a different motion in a first period of time (Fig.III.3.11).

After another period of time one couldn't say considering only the current behaviour of the system, that the two r- values lying so close together.
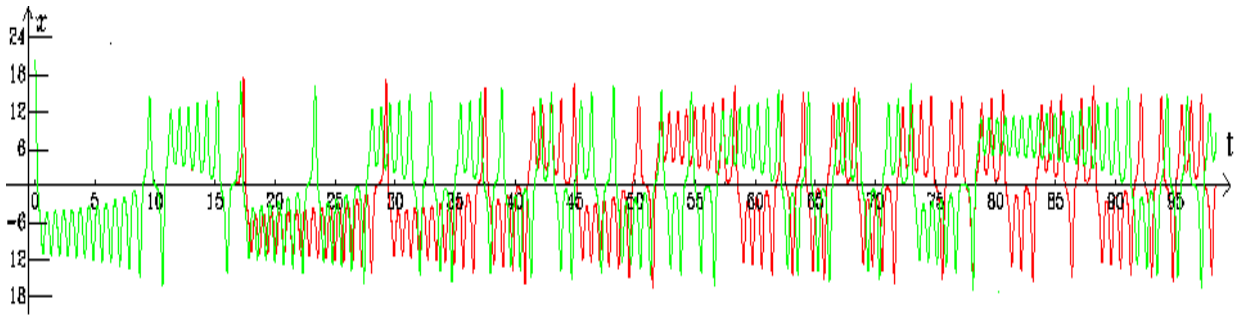

Fig. III.3.11: x as function of t for r = 24.74001 (green line) and r = 24.74 (red line)

The second aspect we want to show is the behaviour of this chaotic system nearby critical points. For these values of r we can choose different initial conditions as we did for r = 24.1, but we always get the same graphs, that is to say butterfly figures, that can also be seen in a 3D diagram (Fig.III.3.12).
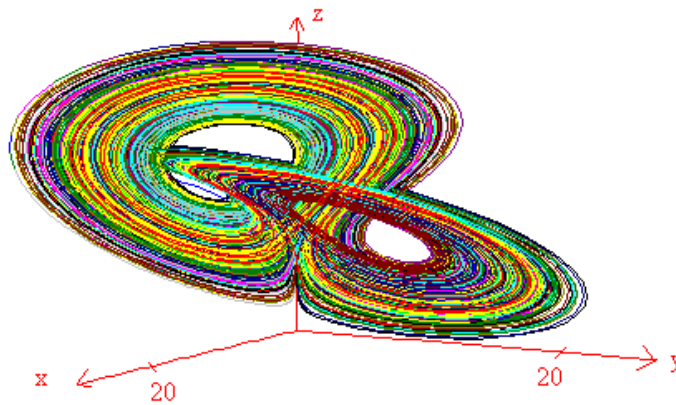

Fig. III.3.12: (x, y, z)- diagram for initial values (x, y, z) = (20, 20, 20) and r = 24.74

This effect when equilibrium points loose their stability and pass into the mentioned spirals is called a Hopf bifurcation. It occurs in damped systems where small disturbances decay after a certain time. In the Lorenz system this decay rate depends on the parameter r. At a critical value the decay rate changes into growth and thus equilibrium states loose their stability. One can calculate the exact critical value of r where this bifurcation happens by regarding the Jacobian matrix of the Lorenz system:

$$ J = \begin{vmatrix} \dfrac{\partial\,\dot{x}}{\partial\,x} & \dfrac{\partial\,\dot{x}}{\partial\,y} & \dfrac{\partial\,\dot{x}}{\partial\,z} \\ \dfrac{\partial\,\dot{y}}{\partial\,x} & \dfrac{\partial\,\dot{y}}{\partial\,y} & \dfrac{\partial\,\dot{y}}{\partial\,z} \\ \dfrac{\partial\,\dot{z}}{\partial\,x} & \dfrac{\partial\,\dot{z}}{\partial\,y} & \dfrac{\partial\,\dot{z}}{\partial\,z} \end{vmatrix} = \begin{pmatrix} -s & s & 0 \\ r-z & -1 & -x \\ y & x & -b \end{pmatrix} \tag{III.3.8} $$

Now the eigenvalue (λ) equation can be written as:

$$\lambda^3 + \lambda^2\,(s + b + 1) + \lambda\,b\,(s + r) + 2sb\,(r\text{-}1) = 0 \qquad\qquad \text{(III.3.9)}$$

This equation has the solutions (obtained by a complex approach):

$$\lambda_1 = 0 \text{ and } \lambda_{2/3} = \pm\, i\omega \qquad\qquad\qquad \text{(III.3.10)}$$

With $\lambda_1 = 0$, we get:

$$2sb * (r\text{-}1) = 0 \qquad\Rightarrow\qquad r = 1 \qquad\qquad \text{(III.3.11)}$$

For λ_1 we get a pitchfork bifurcation that we have also discussed in an earlier section.

That's why we want to study the cases $\lambda_{2/3} = \pm\, i\omega$ and precisely $\lambda_2 = + i\omega$ because it's the same calculus for both values as one can easily reproduce.

$$-i\,\omega^3 - \omega^2\,(s + b + 1) + i\omega\,(s + r) + 2sb\,(r\text{-}1) = 0 \qquad\qquad \text{(III.3.12)}$$

Separating the imaginary and the real part we get:

$$\omega^2 = b(s + r) \text{ and } \omega^2 = \frac{2sb * (r - 1)}{(s + b + 1)} \qquad\qquad \text{(III.3.13)}$$

$$\Rightarrow\qquad r = \frac{s(s+b+3)}{s - b - 1} = r_H$$

For the standard values $b = 8/3$ and $s = 10$ we get: $r_H \approx 24,7368$. It means that for $r > r_H$ we always get – independent of the initial conditions – stable spirals around the two stable points calculated above. The difference between the behaviour for different large r – values is only the frequency of changing between the spirals around their own two attractive points. In phase space you see the famous butterfly pictures. They present the Lorenz attractor.

An attractor is characterized by two properties: Trajectories starting in A remaining there and A attracts an open set of initial conditions, that means every path starting in the stability range of the attractor approaches arbitrarily every point of the attractor. But the Lorenz attractor is a strange attractor that means it has a non whole-number dimension and attraction is very sensible to small perturbations, as we have seen in our observations. Lorenz called it strange because trajectories are bounded and nevertheless there are no stable points.

But the r variation effects also multiple chaotic effects we have studied closer in the section. Hence we can establish, that chaotic systems described by nonlinear differential equations are also sensitive to small changes of parameters. It is rather a composition of initial conditions and parameters that cause all facets of chaotic behaviour.

III.4 Van der Pol oscillator

III.4.1 Introduction

As we have seen during the first experiments, oscillations appear in electric phenomena. Also one of the more interesting experiments is the Van der Pol oscillator.

The *Van der Pol lamp generator circuit* (see fig. III.4.1) is a self-sustained oscillatory system. The **damped oscillation** is given by the LCR circuit (red) and its **source of energy** is the anode current (green). The system influences the inductive coil (blue), while the nonlinear effects of this can be seen by the behaviour of the triode lamp (brown).

The Van der Pol equation describes the voltage between points P_1 and P_2. Using dimensionless variables, this equation can be written as

(c) 2006 by Joachim Franck

Fig. III.4.1: Van der Pol lamp generator circuit

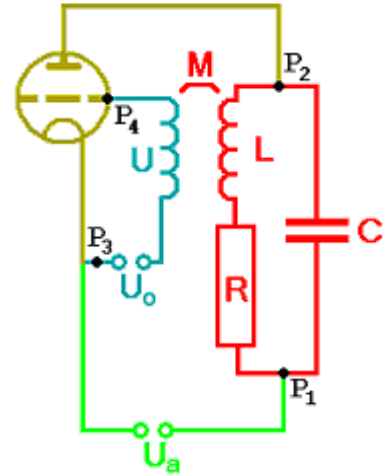$$\frac{d^2 x}{d\tau^2} + a \cdot (x^2 - 1) \cdot \frac{dx}{d\tau} + x = 0 \quad , \tag{III.4.1}$$

a nonlinear, homogeneous, second-order differential equation.

The forced Van der Pol oscillator is analogous described by this inhomogeneous equation:

$$\frac{d^2 x}{d\tau^2} + a \cdot (x^2 - 1) \cdot \frac{dx}{d\tau} + x = A \cdot \sin(\Omega \cdot t) \tag{III.4 .2}$$

Using higher order polynomials, e.g. having a better approximation, equation (III.4.1) turns to

$$\frac{d^2 x}{d\tau^2} + \alpha \cdot (\theta \cdot x^4 + \beta \cdot x^2 - 1) \cdot \frac{dx}{d\tau} + x = 0 \quad . \tag{III.4 .3}$$

III.4.2 Small Amplitude oscillations

Using $v = \dfrac{dx}{d\tau}$ we can write our equation (III.4.1) as two first-order functions:

$$f_1(x,v) = v = \dot{x}$$

$$f_2(x,v) = \dot{v} = a \cdot v \cdot (1 - x^2) - x$$

Setting both functions equal to zero we easily obtain x=0 and v=0 for the fixed point. (Compare: Hilborn, "Chaos and Nonlinear Dynamics", Oxford University Press, 2000)

If we set *a*=0 in equation III.4.1 our system turns to a simple harmonic oscillator. Physically it means that the blue circuit in figure III.4.1 as well as the resistor just does not exist.

In phase space, this simple system describes a circle with constant radius. In (t,x)-diagram, it describes a sine curve.

Changing initial conditions of the system, the radius of our phase space trajectory also changes: the larger x(t=0) or v(t=0) are, the longer it is – we can see concentric cycles with starting points depending on initial conditions.
(see fig. III.4.2).

Fig. III.4.2: Phase space portrait for a=0 and different initial values of x_0 and v_0:
black curve: $x_0 = 1$; $v_0 = 0$
blue curve: $x_0 = 2$; $v_0 = 0$
red curve: $x_0 = 3$; $v_0 = 0$
green curve: $x_0 = 4$; $v_0 = 0$

Setting a to a nonzero value, phase space trajectories distort from a circle. The larger a is, the less the trajectory looks like a circle (see fig. III.4.3). This makes sense because x0 is some kind of potential energy and v0 the system's kinetic energy. Both are quadratic forms and the sum of them is the system's total energy, e.g. the area of the circle in phase space portrait
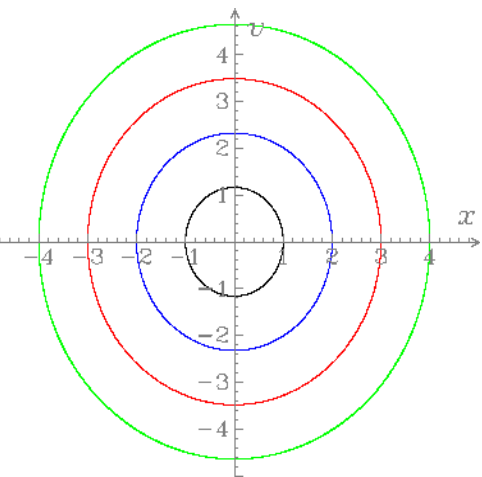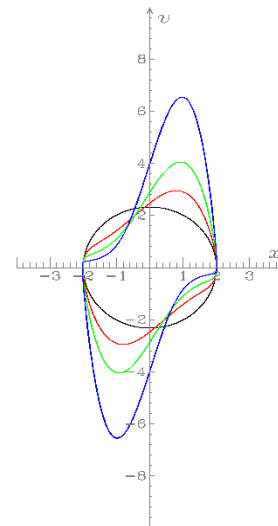
Fig. III.4.3: Phase space prtrait for constant initial values but different values of a *(black: 0; red: 1; green: 2; blue:3).*

30

The more interesting fact is that now the phase space portrait is independent of the system's initial conditions – *all* trajectories (nonzero initial conditions) are attracted to this curve called *limit cycle:* The trajectories start away from this curve but are attracted by it.

Physically the system's energy dissipation (friction) now depends on the deviation of *x* and can sometimes be *less than zero* implicating that the system absorbs energy from its source. Of course, the system can only be stable if it dissipates energy when it has too much of it and absorbs energy when it has too little. We obtain a self-sustained oscillator as we discussed in the introduction.
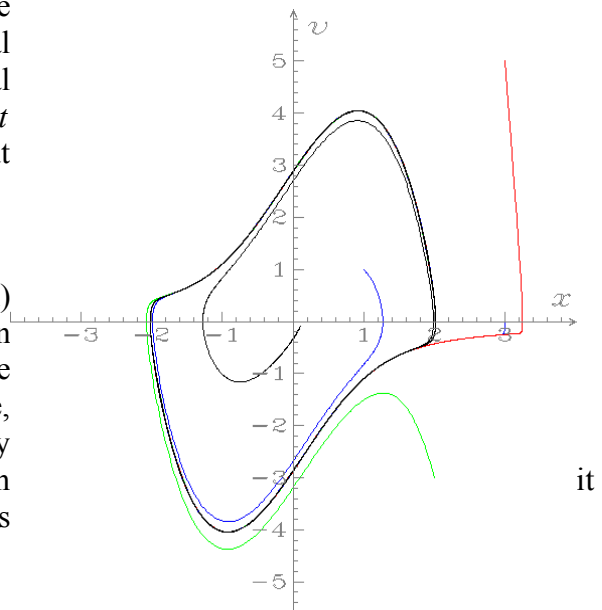
Fig. III.4.4: The limit cycle attracts the trajectories independent from the system's initial conditions (a = 1).
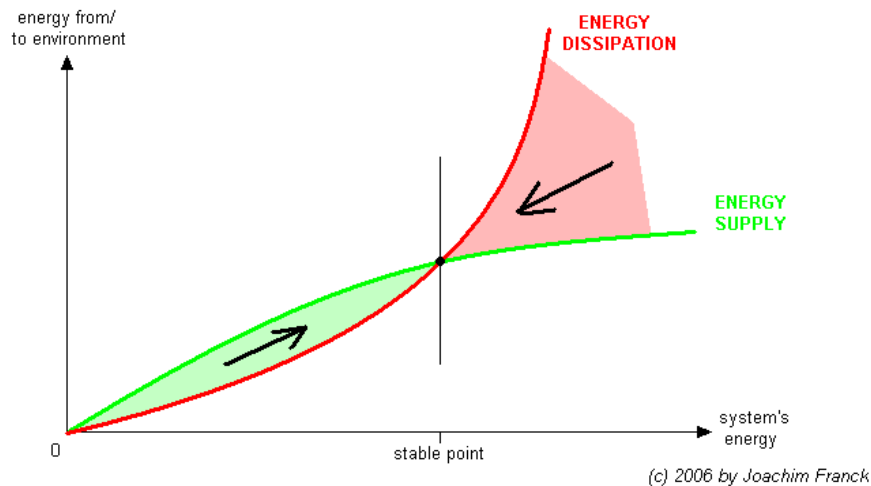
Fig. III.4.5: This sketch illustrates the stability of a self-sustained oscillator. Starting from a state different from the stable one or being disturbed, the system returns to its characteristic motion.

As any other self-sustained oscillators, the Van der Pol oscillator's form of motion is entirely described by the internal parameter(s), here $a \neq 0$, but independent from initial conditions (see above). An explicit time-dependent value does not appear, implicit a is time-dependent: when the anode current source expires, *a* remains less than zero and the oscillation slows down.

31

III.4.3 Relaxation oscillations

  As we saw, the higher *a* is chosen, the more the phase space portrait distorts from a circle. Plotting (t, x)-diagram we see that the system's movement is periodic but doesn't have the form of a sine: Analogous to its phase space portrait (see fig. III.4.3 or III.4.4), the higher *a* is chosen, the more the time course looks like a kind of a *saw tooth curve* (or *shark's fin curve*) because of the speed-dependent energy dissipation.
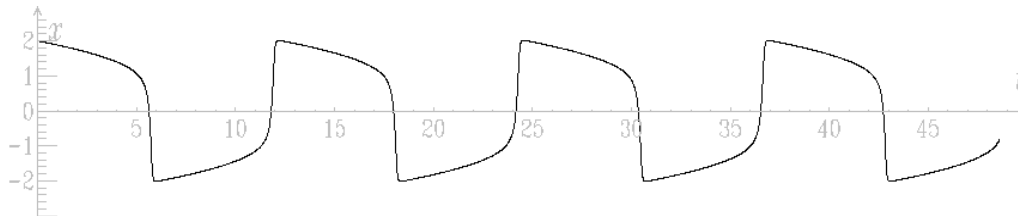

Fig. III.4.6: Time-dependence of x *(*a = 5; x_0 = 2; v_0 = 0*).*

III.4.4 Hard Excitation

  Including higher order polynomials is necessary if one wants a better approximation of the real system's behaviour – see equation (III.4 .2). Now the system appears to have two different attractors: a limit cycle comparable with the cycles above and the origin of the phase space – it completely dissipates its energy (hard excitation). Between them there is an instable state called repulsor or repellor (and has to be as being between two attractors), which could – in other systems – also be a point just like the inner attractor in this case.

Fig. III.4.7a (right): Phase space portrait for
$\alpha = -0.1; \beta = 20; \theta = -27$
and various initial conditions

Red, black and green curve: Here every movement of the system is quickly inhibited because of strong speed-dependent damping. The trajectories of these combinations of initial conditions spiral to the same limit cycle.

Blue curve: Here the system absorbs energy until it reaches its limit cycle. It is easy to see that this limit cycle is the same as before.

The purple curve is attracted by the origin of phase space, a behavior that didn't appear until now. In section IV.2.1 the trajectories were only deflected by it (see fig. 4).
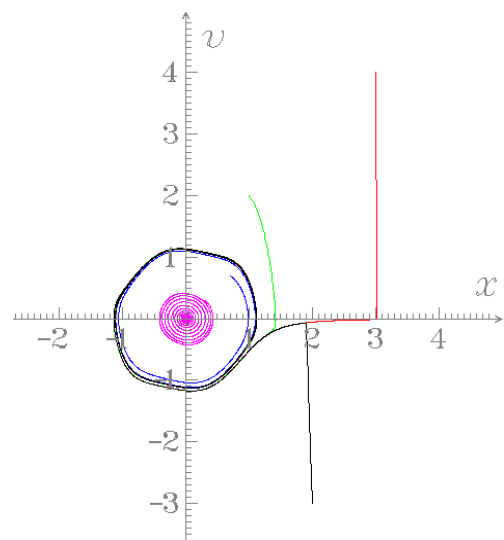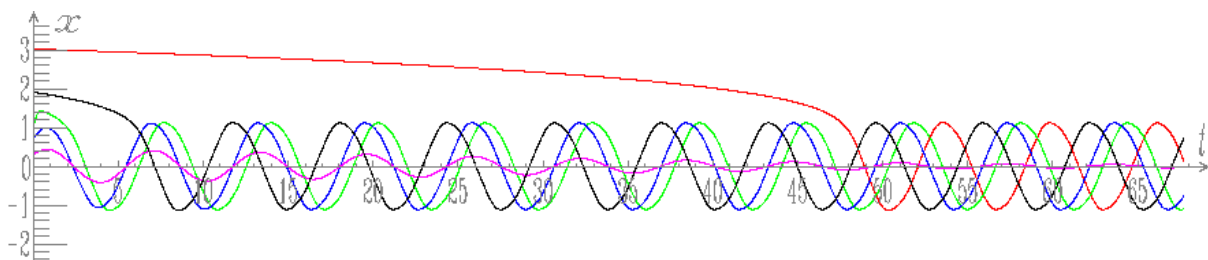
Fig. III.4.7b: The same movements, but plotted as functions x(t).

32

To examine the repulsor's shape in phase space we set the initial speed v_0 to zero and watch the trajectory's behaviour in dependence of the initial deviation x_0. So we explored that the repulsor crosses the *x*-axis at about 0.48824.
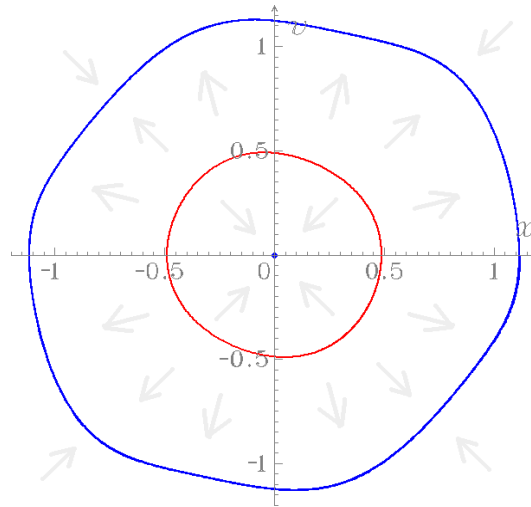

Fig. III.4.8: Attractors (blue: $x_0 = 0$ resp. $x_0 = 1.2$) and the repulsor (red: $x_0 \approx 0.49$) of the hard excited Van der Pol system. The grey arrows symbolize the trajectories' movement. The repulsor describes an instable state: After some time a nearby trajectory either spirals in or out to approach the nearest attractor.

III.4.5 Synchronization

Fixing the parameters of the system but driving it by a periodic force (equation III.4.3) we find another interesting feature of the Van der Pol system – synchronization. If one varies amplitude and frequency of the external force, it comes out that there are three different cases of the system's behaviour to distinguish, "too weak, too slow", "too weak, too fast", and "locking", where *fast* and *slow* refer to the frequency and *weak* to the amplitude of the external force. Locking occurs when the amplitude of the force is high enough and its frequency does not differ too much from the system's natural frequency. The other two cases – non-locking – appear to be similar in system's behaviour.
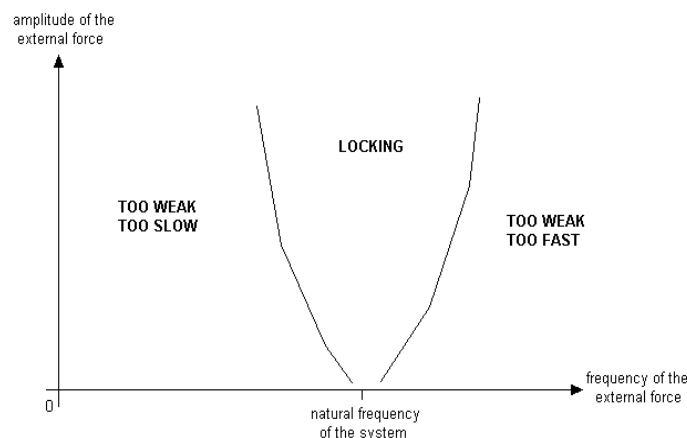

Fig. III.4.9: This sketch illustrates the system's behavior in dependence of the two parameters of the external force. (Compare: Arnol'd tongue *in Argyris/Faust/Haase „Die Erforschung des Chaos", Vieweg, 1994; Hao Bai-Lin: „Chaos", World Scientific Singapore, 1984)*

33

The non-locking case is easily recognizable in phase space and deviation-force-diagram. Both curves never stay stationary – phase space trajectory varies around the natural (e.g. not forced) trajectory while in deviation-force-diagram nearly every combination of the system's and force's deviation seem to be possible.
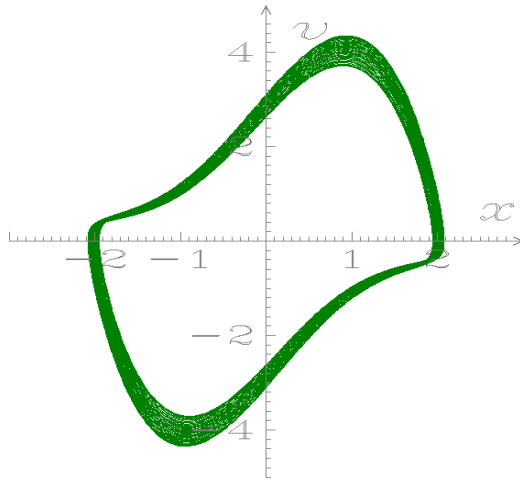

Fig. III.4.10a: phase space diagram of a Van der Pol oscillator being forced too weak and too slow to be locked
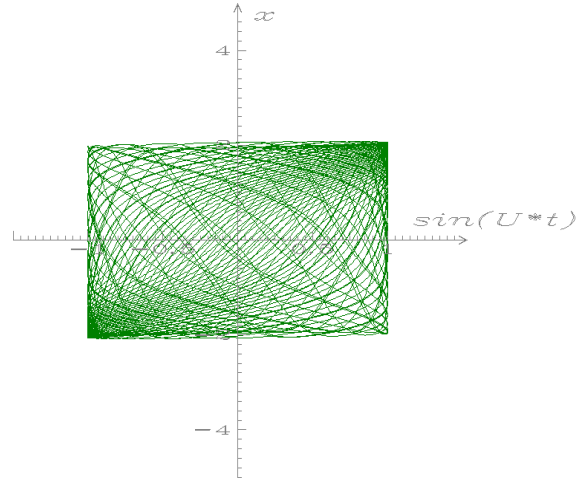

Fig. III.4.10b: The same process. The system's deviation is plotted in dependence of the force's relative deviation (U = Ω).

While non-locking is comparable with a damped, harmonic oscillator which is driven by a periodic force with a frequency different from the system's natural frequency, locking is the analogon to resonance. Aside from the fact that the amplitude of the Van der Pol system does not change significantly, the two other properties of resonance appear here, too:

– locking frequency is nearby the system's natural frequency

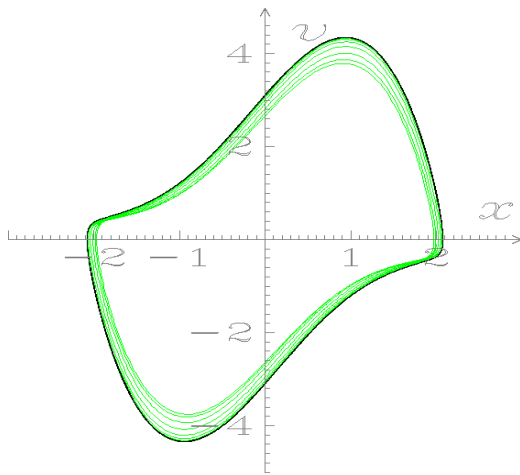– there is a phase shift between force and system of approximately $\dfrac{\pi}{2}$

Fig. III.4.11a: Phase space diagram of a Van der Pol oscillator being locked. After some time (transient, green) the system's trajectory stays stationary.
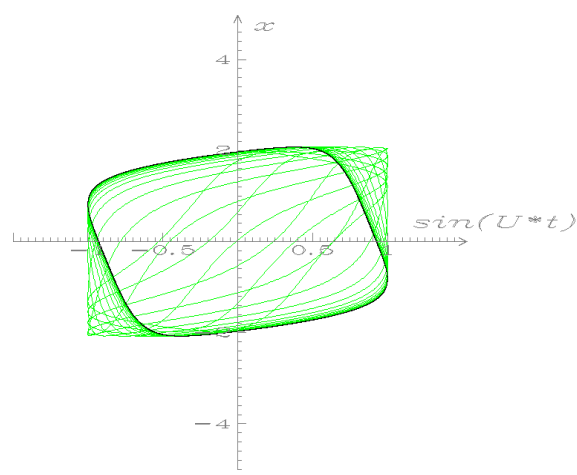

Fig. III.4.11b: The same process. In stationary state (black curve) the system runs through a cycle in positive direction, so there is a phase shift of π/2 between force and system (U = Ω).

System and force need not have this phase shift from the start because the force prolongs the system's period slightly as long as the phase shift between them is not $\pi/2$. As we saw, this can only happen if their periods (frequencies) are not too different, otherwise the period just can not be changed *slightly*. If the system's natural frequency and the force's one differ, but not more than the same *slightly*, the force pulls (or pushes) the system continuously to maintain the same frequency and constant phase shift.
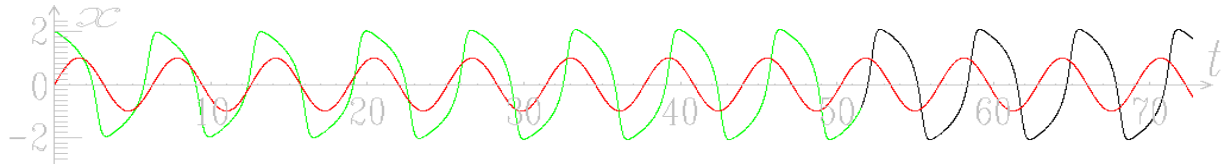
Fig. III.4.12: The system's behavior as a function of time. The red curve is the relative force, green is the system's deviation while transient, black in stationary state.

III.4.6 Conclusion

From the first sight, it is hard to imagine that such a simple differential equation like Van der Pol's contains so many interesting features. But unforeseeable behaviour, self sustained oscillations, attractors and repulsors, transients and synchronization are not only features of the Van der Pol system, they are main topics of chaos theory. So, studying this lamp generator can help us to understand other oscillating chaotic systems: heartbeat, clock synchronization, planet systems and many more.

IV General Conclusion

No matter where one starts from – electricity, mechanics, motion of fluids – you always come to this topic: chaos.

At the beginning we analyzed electrical circuits and their elements: resistors, coils, capacitors. These circuits were not difficult enough to cause significant chaotic behaviour, but helped us to understand how their elements work.

After that we dealt with two mechanical chaotic systems: the double pendulum and the Lorenz system. We studied how chaotic behaviour is determined by the system's physical parameters. It came out that some systems can not even be described mathematically because their differential equations of movement can not be solved (integrated). Even if some systems can be modelled, it does not mean that they are described correctly because rounding errors always appear. But sometimes also nearby phase space trajectories of the system diverge after some time and this is not caused by rounding but by nature – the nature of chaos.

Dealing with the Van der Pol oscillator simulation, we learned a lot about some special features of nonlinearity. Its behaviour was easier to manipulate than the Lorenz' one and it could have been interesting if we implemented this simulation in reality.

V Appendix - Charging and discharging a capacitor

This table shows in detail the capacitor's voltage in dependence of time (fig. II.2.3).

Time (sec)	Voltage (V)	Time (sec)	Voltage (V)	Time (sec)	Voltage (V)
1	0,53	34	4,75	67	1,04
2	0,92	35	4,76	68	0,96
3	1,27	36	4,8	69	0,88
4	1,61	37	4,82	70	0,80
5	1,90	38	4,82	71	0,75
6	2,16	39	4,84	72	0,69
7	2,41	40	4,86	73	0,63
8	2,63	41	4,86	74	0,59
9	2,82	42	4,88	75	0,55
10	3,00	43	4,90	76	0,49
11	3,18	44	4,90	77	0,45
12	3,33	45	4,90	78	0,41
13	3,49	46	4,92	79	0,39
14	3,61	47	4,92	80	0,35
15	3,75	48	4,94	81	0,33
16	3,84	49	4,94	82	0,31
17	3,92	50	4,59	83	0,29
18	4,02	51	4,20	84	0,25
19	4,10	52	3,82	85	0,25
20	4,18	53	3,51	86	0,22
21	4,24	54	3,20	87	0,22
22	4,31	55	2,92	88	0,20
23	4,37	56	2,69	89	0,18
24	4,43	57	2,45	90	0,18
25	4,47	58	2,25	91	0,18
26	4,51	59	2,06	92	0,16
27	4,55	60	1,90	93	0,16
28	4,59	61	1,73	94	0,14
29	4,63	62	1,59	95	0,12
30	4,65	63	1,47	96	0,12
31	4,69	64	1,33	97	0,10
32	4,71	65	1,22		
33	4,73	66	1,14		

VI References

Dynamical systems and numerical analysis, A.M. Stuart and A.R. Humphries, Cambridge University Press, Cambridge, 1998

Die Physisk des Wetters und des Klimas, Hans Joachim Lange, Reimer, Berlin, 2002

Nonlinear Dynamics and Chaos, Steven H. Strogatz, Westview, Cambridge, 1994

Nonlinear Dynamics, M. Lakshmanan and S. Rajasekar, Springer, Berlin, 2003

wikipedia.org (visited in december 2006)